Nucleon-to-Delta axial transition form factors in relativistic baryon chiral perturbation theory

L. S. Geng, J. Martin Camalich, L. Alvarez-Ruso, and M. J. Vicente Vacas

Departamento de Física Teórica and IFIC,

Centro Mixto Universidad de Valencia-CSIC,

Institutos de Investigación de Paterna,

Aptdo. 22085, 46071 Valencia, Spain

(Dated: February 17, 2013)

Abstract

We report a theoretical study of the axial Nucleon to Delta(1232) ($N \to \Delta$) transition form factors up to one-loop order in relativistic baryon chiral perturbation theory. We adopt a formalism in which the Δ couplings obey the spin-3/2 gauge symmetry and, therefore, decouple the unphysical spin-1/2 fields. We compare the results with phenomenological form factors obtained from neutrino bubble chamber data and in quark models.

PACS numbers: 23.40.Bw,12.39.Fe, 14.20.Gk

I. INTRODUCTION

The axial $N \to \Delta(1232)$ transition form factors play an important role in neutrino induced pion production on the nucleon, in particular at low energies [1, 2, 3, 4, 5]. These form factors have been parametrized phenomenologically to fit the ANL [6, 7] and BNL [8, 9] bubble-chamber data. In the past, the theoretical descriptions have been done using different approaches, for a review, see Ref. [10]. In recent years, there has been an increasing interest on these form factors. They have been calculated, for instance, using the chiral constituent quark model [11] and light cone QCD sum rules [12]. State of the art calculations within lattice QCD [13, 14] have also become available. The possibility to extract the axial $N \to \Delta$ transition form factors using parity-violating electron scattering at Jefferson Lab [15] has been studied extensively [16, 17]. Present and future neutrino experiments could also provide further information on these form factors [18, 19, 20, 21, 22, 23].

Chiral perturbation theory, based on a simultaneous expansion of QCD Green functions in powers of the external momenta and of the quark masses, has achieved remarkable success in describing the dynamics of the light pseudoscalar mesons at low energies [24, 25, 26, 27]. The sector with one baryon is more problematic because, as was shown in Ref. [28], the systematic power counting is lost since the nucleon mass is not zero in the chiral limit. These problems were first handled in heavy baryon chiral perturbation theory (HBχPT), where nucleons are treated semi-relativistically [29, 30]. However, in certain cases, this approximation leads to convergence problems because the Green functions do not satisfy the analytical properties of the fully relativistic theory [31]. Recently, the systematic power counting has also been restored in the relativistic formulation through either the infrared [31] or the extended on-mass-shell regularization schemes [32, 33].

The explicit inclusion of the Δ in chiral perturbation theory requires a power counting that properly incorporates the Δ-N mass difference, $\Delta \equiv M_\Delta - M_N$, which is small compared to the chiral symmetry breaking scale. Two expansion schemes have been proposed. One is the small scale expansion [34] which considers Δ to be of the same order as the other small scales in the theory, i.e., $m_\pi \sim p \sim \Delta$. The other is the δ expansion scheme, which counts Δ differently depending on the energy domain [35]. Originally, the small scale expansion was used in HBχPT, while recently it has also been implemented in relativistic chiral perturbation theory [36, 37].

The vector $N \to \Delta$ transition form factors, important to understand eN (γN) reactions and the structure of the nucleon, have been calculated up to next-to-leading order in both the small scale expansion HBχPT [38, 39] and the δ expansion relativistic baryon χPT [40, 41]. While axial form factors have been addressed in HBχPT [42], no calculation has been performed up to now within the relativistic framework. With lattice QCD results becoming available [13], it is timely to study the axial transition form factors within relativistic chiral perturbation theory.

In this paper, we use the relativistic baryon chiral perturbation theory, including explicitly the Δ resonance, to calculate the axial $N \to \Delta$ transition form factors up to order 3 in the δ expansion. In sect. II, we briefly explain the power counting, the difference between the small scale expansion scheme and the δ expansion scheme, write down the relevant Lagrangians up to next-to-next-to-leading order and the appropriate form of the Δ propagator. Loop calculations are performed in sect. III. In sect. IV, we discuss our results in terms of the low energy constants and loop functions. In sect. V we compare the results with both phenomenological parameterizations and other theoretical calculations. Summary and conclusions are given in sect. VI.

II. POWER COUNTING, EFFECTIVE LAGRANGIANS, AND THE Δ PROPAGATOR

A. Power counting

A fundamental concept of χPT (as Effective Field Theory) is the power counting [24]. It provides a systematic organization of the effective Lagrangians and the corresponding loop-diagrams within a perturbative expansion in powers of $(p/\Lambda_{\chi\mathrm{SB}})^{n_{\chi PT}}$, where p is a small momentum or scale and $\Lambda_{\chi\mathrm{SB}}$, the chiral symmetry breaking scale. In χPT with pions and nucleons alone the chiral order of a diagram with L loops, $N_\pi(N_N)$ pion (nucleon) propagators, and V_k vertices from kth-order Lagrangians is

$$n_{\chi PT} = 4L - 2N_\pi - N_N + \sum_k k V_k \,. \tag{1}$$

However, in the covariant theory this rule is violated in loops by lower-order analytical pieces [28]. This power counting can be recovered by adopting non-trivial renormalization

schemes, where the lower-order power-counting breaking pieces of the loop results are systematically absorbed into the available counter-terms [31, 33]. A detailed discussion of the renormalization scheme adopted in the present work will be presented together with our main results in section IV.

If the Δ resonance is explicitly considered, things become more complicated because its excitation energy, $\Delta \equiv M_\Delta - M_N \sim 0.3\,\mathrm{GeV}$, is small compared to the chiral symmetry breaking scale $\Lambda_{\chi\mathrm{SB}} = 4\pi f_\pi \sim 1\,\mathrm{GeV}$. Therefore, there are two small parameters in the theory, i.e.,

$$\varepsilon = m_\pi/\Lambda_{\chi\mathrm{SB}} \quad \text{and} \quad \delta = \Delta/\Lambda_{\chi\mathrm{SB}}. \tag{2}$$

Over the past few years, two different expansion schemes have been proposed, the small scale expansion and the δ expansion. In the small scale expansion [34], one has $m_\pi \sim \Delta \sim p \sim \mathcal{O}(\epsilon)$. In the δ-expansion [35], to maintain the scale hierarchy $m_\pi \ll \Delta \ll \Lambda_{\chi\mathrm{SB}}$, $m_\pi/\Lambda_{\chi\mathrm{SB}}$ is counted as δ^2. In this scheme, the power counting depends on the energy domain under study: $p \sim m_\pi$ or $p \sim \Delta$.

For the study of $N \to \Delta$ axial transition form factors in the energy region $p \sim \Delta$, the order of a graph with L loops, V_k vertices of dimension k, N_π pion propagators, N_N nucleon propagators, N_Δ Delta propagators, the power-counting index n is given by:

$$n = n_{\chi\mathrm{PT}} - N_\Delta. \tag{3}$$

For a more general discussion, see Ref. [43].

In the present work, we adopt the δ expansion scheme. As can be seen in the following sections, the differences between these two schemes in our case come from vertices proportional to m_π^2, which count as δ^4 in the δ expansion and, therefore, have been neglected.

B. Chiral Lagrangians

In this section, we write down the relevant NN, $N\Delta$, and $\Delta\Delta$ Lagrangians and pay special attention to the Δ couplings and the spin-3/2 gauge symmetry.

1. Pion-nucleon and pion-pion Lagrangians

The lowest order pion-nucleon Lagrangian has the following form:

$$\mathcal{L}_{\pi N}^{(1)} = \bar{N}(i\gamma^\mu D_\mu - M_N - \frac{g_A}{2}\gamma^\mu\gamma^5 u_\mu)N, \tag{4}$$

where M_N and g_A are the nucleon mass and the axial-vector coupling at the chiral limit, D_μ is the covariant derivative

$$D_\mu N = \partial_\mu N + [\Gamma_\mu, N], \tag{5}$$

$$\Gamma_\mu = \frac{1}{2}\left\{u^\dagger(\partial_\mu - ir_\mu)u + u(\partial_\mu - il_\mu)u^\dagger\right\}, \tag{6}$$

and u_μ the axial current defined as

$$u_\mu = i\left\{u^\dagger(\partial_\mu - ir_\mu)u - u(\partial_\mu - il_\mu)u^\dagger\right\}. \tag{7}$$

In the above definitions, $r_\mu = v_\mu + a_\mu$, $l_\mu = v_\mu - a_\mu$ with $v_\mu = \tau^\sigma v_\mu^\sigma/2$ and $a_\mu = \tau^\sigma a_\mu^\sigma/2$ the external vector and axial currents, where τ^σ are the Pauli matrices. The matrix u incorporates the pion fields

$$u^2 = U = \exp\left[i\frac{\Phi}{f_\pi}\right], \tag{8}$$

$$\Phi = \tau_\sigma\pi^\sigma = \begin{pmatrix} \pi^0 & \sqrt{2}\pi^+ \\ \sqrt{2}\pi^- & -\pi^0 \end{pmatrix}, \tag{9}$$

with f_π being the pion decay constant in the chiral limit.

The leading order pion-pion Lagrangian has the following form:

$$\mathcal{L}_{\pi\pi}^{(2)} = \frac{f_\pi^2}{4}\mathrm{Tr}\left[\nabla_\mu U(\nabla^\mu U)^\dagger\right] + \frac{f_\pi^2}{4}\mathrm{Tr}\left[\chi U^\dagger + U\chi^\dagger\right], \tag{10}$$

where

$$\nabla_\mu U = \partial_\mu U - ir_\mu U + iUl_\mu \tag{11}$$

with $\chi = \mathrm{diag}(m_\pi^2, m_\pi^2)$.

2. Nucleon-Delta and Delta-Delta Lagrangians

The $\Delta(1232)$ is a spin-3/2 resonance and, therefore, its spin content can be described in terms of the Rarita-Schwinger (RS) field Δ_μ, where μ is the Lorentz index.[1] This field,

[1] We follow Ref. [43] and write the Lagrangians for the spin-3/2 isospin-3/2 Δ isobar in terms of the Rarita-Schwinger (vector-spinor) isoquartet field $\Delta_\mu = (\Delta^{++}, \Delta^+, \Delta^0, \Delta^-)_\mu^t$, which is connected to the

however, contains unphysical spin-1/2 components. They are allowed for the description of off-shell Delta's, but the physical results should not depend on them. In order to tackle this problem, we follow Refs. [43, 45] and adopt the *consistent* couplings, which are gauge-invariant under the transformation

$$\Delta_\mu(x) \to \Delta_\mu(x) + \partial_\mu \epsilon(x). \tag{12}$$

A remarkable consequence of the use of the spin-3/2 gauge symmetric couplings is that it leads to a natural decoupling of the propagation of the spin-1/2 fields.

In the following we give the $N\Delta$ and $\Delta\Delta$ Lagrangians relevant to this work. The lowest order Lagrangians in the resonance region are[2]

$$\mathcal{L}^{(1)}_{N\Delta} = -\frac{ih_A}{2M_\Delta}\bar{N}T^a\gamma^{\mu\nu\lambda}(\partial_\mu\Delta_\nu)\omega^a_\lambda + \text{H.c.}, \tag{13}$$

$$\mathcal{L}^{(1)}_{\Delta\Delta} = \frac{H_A}{2M^2_\Delta}\partial_m\bar{\Delta}_b\gamma^{\ell bm}\gamma^\mu\gamma^5\mathcal{T}^a\omega^a_\mu\gamma_{\ell cn}\partial^n\Delta^c, \tag{14}$$

where $\omega^a_\lambda = \frac{1}{2}\text{Tr}\,(\tau^a u_\lambda) = -\frac{1}{f_\pi}\partial_\lambda\pi^a + a^a_\lambda + \cdots$, T^a and $\mathcal{T}^a$ are the isospin 1/2 to 3/2 and 3/2 to 3/2 transition matrices, and $\gamma^{\mu\nu\lambda}$ is the totally antisymmetric gamma matrix product as given in Appendix A. At second order, there are four terms, i.e.,[3]

$$\begin{aligned}\mathcal{L}^{(2)}_{N\Delta} \;=\; & -\frac{d_1}{M_\Delta}\bar{N}T^a(\partial_\mu\Delta_\nu)f^{a,\mu\nu}_- - id_2\bar{N}T^a f^{a,\mu\nu}_-\gamma_\mu\Delta_\nu - id_3\bar{N}T^a\omega^{a,\mu\nu}\gamma_\mu\Delta_\nu \\ & -\frac{d_4}{M_\Delta}\bar{N}T^a(\partial_\mu\Delta_\nu)\omega^{a,\mu\nu} + \text{H.c.},\end{aligned} \tag{15}$$

---

isospurion representation of Ref. [34] through

$$\Delta^a_\mu = -T^a\Delta_\mu$$

where T^a are the isospin 1/2 to 3/2 matrices satisfying $T^aT^{b\dagger} = \delta^{ab} - 1/3\tau^a\tau^b$, as given in Appendix A. With this rule, the on-shell equivalent form of our *consistent* couplings can be easily identified with those of Refs. [34, 44].

[2] If one Δ is put on-shell, the Δ-Δ Lagrangian is equivalent to that of Pascalutsa et al. [43]:

$$\mathcal{L}^{(1)}_{\Delta\Delta} = -\frac{H_A}{2M_\Delta}\epsilon^{\mu\nu\rho\sigma}\bar{\Delta}_\mu\mathcal{T}^a(\partial_\rho\Delta_\nu)\omega^a_\sigma + \text{H.c.}.$$

[3] In our study of the axial form factors up to one-loop order the $\delta^{(2)}$ and $\delta^{(3)}$ Lagrangians only concern on-shell Δ's. Therefore, they are the same in the *consistent* coupling scheme of Pascalutsa et al. as those conventional Lagrangians in Refs. [34, 44].

while at third order, there are seven terms[4]

$$\begin{aligned}\mathcal{L}^{(3)}_{N\Delta} \;=\; & -f_1\bar{N}T^a\Delta_\nu\partial_\mu f_-^{a,\mu\nu} - f_2\bar{N}T^a\Delta_\nu\partial_\mu\omega^{a,\mu\nu} + i\frac{f_3}{M_\Delta}\bar{N}T^a\partial^\mu f_-^{a,\alpha\nu}\gamma_\nu\partial_\mu\Delta_\alpha \\ & + i\frac{f_4}{M_\Delta}\bar{N}T^a\partial^\mu f_-^{a,\alpha\nu}\gamma_\mu\partial_\nu\Delta_\alpha - i\frac{f_5}{M_\Delta}\bar{N}T^a\partial^\mu\omega^{a,\nu\alpha}\gamma_\mu\partial_\nu\Delta_\alpha \\ & + \frac{f_6}{M_\Delta^2}\bar{N}T^a\partial^\mu f_-^{a,\nu\alpha}\partial_\mu\partial_\nu\Delta_\alpha + \frac{f_7}{M_\Delta^2}\bar{N}T^a\partial^\mu\omega^{a,\nu\alpha}\partial_\mu\partial_\nu\Delta_\alpha + \text{H.c.}, \end{aligned} \tag{16}$$

where $\omega^a_{\mu\nu} = \frac{1}{2}\mathrm{Tr}(\tau^a[D_\mu, u_\nu])$, $f_-^{a,\mu\nu} = \partial^\mu a^{a,\nu} - \partial^\nu a^{a,\mu}$. As we will see later, the $\delta^{(2)}$ and $\delta^{(3)}$ low-energy constants (LEC) contribute to the form factors only in particular combinations; therefore, the number of independent parameters is smaller than the one appearing in the above Lagrangians.

C. Spin-3/2 propagator

The most general spin-3/2 free field propagator in D dimensions has the following form [36, 46]:

$$\begin{aligned}S^{\alpha\beta}(p) \;=\; & \frac{\not{p}+M_\Delta}{M_\Delta^2-p^2}\Bigg[g^{\alpha\beta} - \frac{\gamma^\alpha\gamma^\beta}{(D-1)} + \frac{(1-\zeta)(\zeta\not{p}+M_\Delta)}{(D-1)(\zeta^2p^2-M_\Delta^2)}(\gamma^\alpha p^\beta - \gamma^\beta p^\alpha) \\ & + \frac{(D-2)(1-\zeta^2)p^\alpha p^\beta}{(D-1)(\zeta^2p^2-M_\Delta^2)}\Bigg], \end{aligned} \tag{17}$$

where ζ is the spin-3/2 gauge-fixing parameter. In the case of $\zeta = 0$, the above propagator corresponds to the usual Rarita-Schwinger propagator

$$S^{\alpha\beta}(p) = \frac{\not{p}+M_\Delta}{M_\Delta^2-p^2}\left[g^{\alpha\beta} - \frac{\gamma^\alpha\gamma^\beta}{(D-1)} - \frac{1}{(D-1)M_\Delta}(\gamma^\alpha p^\beta - \gamma^\beta p^\alpha) - \frac{(D-2)p^\alpha p^\beta}{(D-1)M_\Delta^2}\right]; \tag{18}$$

while in the case of $\zeta = \infty$, it becomes

$$S^{\alpha\beta}(p) = \frac{\not{p}+M_\Delta}{M_\Delta^2-p^2}\mathcal{P}^{\alpha\beta}_{3/2}(p) \tag{19}$$

with the covariant spin-3/2 projection operator defined by

$$\mathcal{P}^{\alpha\beta}_{3/2}(p) = g^{\alpha\beta} - \frac{\gamma^\alpha\gamma^\beta}{(D-1)} - \frac{1}{(D-1)p^2}\left(\not{p}\gamma^\alpha p^\beta + p^\alpha\gamma^\beta\not{p}\right) - \frac{(D-4)p^\alpha p^\beta}{(D-1)p^2}. \tag{20}$$

[4] In the small scale expansion scheme, there are two more terms at this order proportional to m_π^2, i.e.,

$$-f_8\bar{N}T^a\omega^a_\nu\mathrm{Tr}[\chi_+]\Delta^\nu - f_9 i\bar{N}T^a\left[D_\nu, \chi^a_-\right]\Delta^\nu,$$

where χ_+ and χ_- are external scalar and pseudoscalar sources.

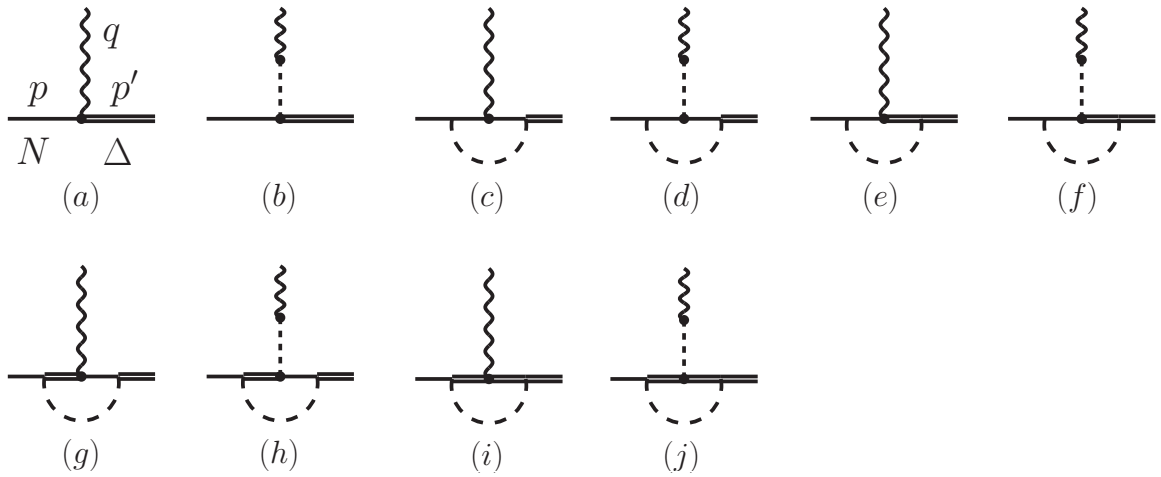

FIG. 1: Feynman diagrams contributing to the axial $N \to \Delta$ transition form factors up to $\delta^{(3)}$. The double, solid, and dashed lines correspond to the Delta, nucleon, and pion, while the wiggly line denotes the external axial source.

It should be stressed that due to the spin-3/2 gauge symmetric nature of the *consistent* couplings, our results do not depend on the particular value of the gauge-fixing parameter ζ.

III. THE $N \to \Delta$ AXIAL TRANSITION FORM FACTORS

The $N \to \Delta$ axial transition form factors can be parameterized in terms of the usually called Adler form factors [1, 47]:

$$\langle \Delta^+_\alpha(p')| - A^{\alpha\mu,3}|P(p)\rangle \;=\; \bar{\Delta}^+_\alpha(p')\Big\{ \frac{C_3^A(q^2)}{M_N}\big(g^{\alpha\mu}\gamma\cdot q - q^\alpha\gamma^\mu\big) + \frac{C_4^A(q^2)}{M_N^2}\big(q\cdot p' g^{\alpha\mu} - q^\alpha p'^\mu\big) + C_5^A(q^2) g^{\alpha\mu} + \frac{C_6^A(q^2)}{M_N^2} q^\alpha q^\mu \Big\} N, \tag{21}$$

where $A^{\alpha\mu,3}$ is the third isospin component of the axial current.

All the diagrams contributing to the $N \to \Delta$ axial transition form factors up to $\delta^{(3)}$ are displayed in Fig. 1.[5] Two Kroll-Ruderman like diagrams are not shown since the one with an internal nucleon and a $A\pi NN$ vertex is zero and the other one with an internal Δ and a

[5] We do not have the diagrams (c), (d), (e), and (f) of Fig. 1 of Ref. [42], that correspond to tadpole diagrams where a pion loop couples to either the $AN\Delta$ ($\pi N\Delta$, $A\pi$) vertices, or the pion fields, because the contribution of those diagrams are of higher-order in the δ expansion scheme.

$A\pi\Delta\Delta$ vertex contributes as a real constant, which is irrelevant to the present study due to the adopted renormalization scheme. The calculation of the tree-level diagrams [Fig. 1(a)] is straightforward:

$$\begin{aligned} A^{\alpha\mu,3}_{(a)} \;=\; \sqrt{\frac{2}{3}}\Bigg[& -\frac{h_A}{2}g^{\alpha\mu} - \frac{d_1}{M_\Delta}(p'\cdot q g^{\alpha\mu} - q^\alpha p'^\mu) - d_2(\gamma\cdot q g^{\alpha\mu} - q^\alpha\gamma^\mu) - d_3\gamma\cdot q g^{\alpha\mu} \\ & -\frac{d_4}{M_\Delta}p'\cdot q g^{\alpha\mu} + f_1(q^2 g^{\alpha\mu} - q^\alpha q^\mu) + f_2 q^2 g^{\alpha\mu} + \frac{f_3}{M_\Delta}p'\cdot q(\gamma\cdot q g^{\alpha\mu} - q^\alpha\gamma^\mu) \\ & +\frac{f_4}{M_\Delta}\gamma\cdot q\,(p'\cdot q g^{\alpha\mu} - q^\alpha p'^\mu) + \frac{f_5}{M_\Delta}\gamma\cdot q p'\cdot q g^{\alpha\mu} + \frac{f_6}{M_\Delta^2}p'\cdot q(p'\cdot q g^{\alpha\mu} - q^\alpha p'^\mu) \\ & +\frac{f_7}{M_\Delta^2}p'\cdot q p'\cdot q g^{\alpha\mu}\Bigg], \end{aligned} \tag{22}$$

where p', p, and q are the momenta of the Δ, the nucleon, and the external source. We assume that both the external nucleon and Δ are on-shell, which yields $p'\cdot q/M_\Delta = (M_\Delta^2 - M_N^2 + q^2)/(2M_\Delta) \approx \Delta$ and $\gamma\cdot q = M_\Delta - M_N = \Delta$, where we have neglected the q^2 and Δ^2 terms which, strictly speaking, are of higher order than the chiral order of the corresponding Lagrangian.

In the following we explicitly show how to calculate the loop diagrams:

Diagram Fig. 1(c) reads

$$A^{\alpha\mu,3}_{(c)} = -\sqrt{\frac{2}{3}}\left[\frac{h_A g_A^2}{(8\pi f_\pi)^2}\frac{1}{M_\Delta}\right] iG^{\alpha\mu}_{(c)} \tag{23}$$

with

$$iG^{\alpha\mu}_{(c)} = (2\pi\mu)^{4-D}\int\frac{d^Dk}{i\pi^2}\frac{p'_b\gamma^{b\alpha c}k_c\,[\not{p}' - \not{k} + M_N]\,\gamma^\mu\gamma_5\,[\not{p} - \not{k} + M_N]\,\not{k}\gamma_5}{[k^2 - m_\pi^2 + i\epsilon][(p-k)^2 - M_N^2 + i\epsilon][(p'-k)^2 - M_N^2 + i\epsilon]}, \tag{24}$$

where μ, the renormalization scale, is set to be M_Δ.

Diagram Fig. 1(e) reads

$$A^{\alpha\mu,3}_{(e)} = \frac{5}{6}\sqrt{\frac{2}{3}}\left[\frac{g_A h_A H_A}{(8\pi f_\pi)^2}\frac{1}{M_\Delta^2}\right] iG^{\alpha\mu}_{(e)}, \tag{25}$$

with

$$iG^{\alpha\mu}_{(e)} = (2\pi\mu)^{4-D}\int\frac{d^Dk}{i\pi^2}\frac{i\epsilon^{\alpha abc}p'_b k_c S_{ad}(p'-k)\gamma^{ed\mu}(p'-k)_e(\not{p} - \not{k} + M_N)\not{k}\gamma_5}{[k^2 - m_\pi^2 + i\epsilon][(p-k)^2 - M_N^2 + i\epsilon]}. \tag{26}$$

Diagram Fig. 1(g) reads

$$A^{\alpha\mu,3}_{(g)} = \frac{1}{6}\sqrt{\frac{2}{3}}\left[\frac{h_A^3}{(8\pi f_\pi)^2}\frac{1}{M_\Delta^3}\right] iG^{\alpha\mu}_{(g)} \tag{27}$$

with

$$iG^{\alpha\mu}_{(g)} = (2\pi\mu)^{4-D}\int\frac{d^Dk}{i\pi^2}\frac{p'_a\gamma^{a\alpha b}k_b(\not{p}'-\not{k}-M_N)\gamma^{c\beta\mu}(p-k)_cS_{\beta\gamma}(p-k)\gamma^{d\gamma e}(p-k)_dk_e}{[k^2-m_\pi^2+i\epsilon][(p'-k)^2-M_N^2+i\epsilon]}. \quad (28)$$

Diagram Fig. 1(i) reads

$$A^{\alpha\mu,3}_{(i)} = \frac{5}{9}\sqrt{\frac{2}{3}}\left[\frac{h_AH_A^2}{(8\pi f_\pi)^2}\frac{1}{M_\Delta^4}\right]iG^{\alpha\mu}_{(i)} \quad (29)$$

with

$$\begin{aligned} iG^{\alpha\mu}_{(i)} &= (2\pi\mu)^{4-D}\int\frac{d^Dk}{i\pi^2} \quad (30)\\ &\times \frac{i\epsilon^{\alpha a\rho\sigma}(p'-k)_\rho k_\sigma S_{ab}(p'-k)\gamma^{lbm}\gamma^\mu\gamma^5\gamma_{lcn}(p'-k)_m(p-k)^nS^{cd}(p-k)\gamma_{fdg}(p-k)^fk^g}{[k^2-m_\pi^2+i\epsilon]}. \end{aligned}$$

In the above equations, $S^{\mu\nu}(p)$ is the spin-3/2 propagator defined in Eq. (17). Since the couplings we used are spin-3/2 gauge symmetric, our results do not depend on the specific value of the gauge fixing parameter.

These loop functions are quite complicated, particularly the ones including Δ internal lines. In practice, we adopt the conventional Feynman parametrization method (see Appendix B) and calculate these loop functions numerically. The manipulation of the Dirac algebra has been performed independently with FORM [48] and FeynCalc [49]. The resulting Feynman parameter integrals are listed in Appendix C. Whenever possible, the numerical results have been checked using the FF library [50] through the LoopTools interface [51].

The one-loop results contain only four different Lorentz structures (due to the constraints $\bar{\Delta}_\alpha\gamma^\alpha = 0$ and $\bar{\Delta}_\alpha p'^\alpha = 0$), i.e., $\gamma^\mu q^\alpha$, $q^\alpha p'^\mu$, $g^{\alpha\mu}$, and $q^\alpha q^\mu$. In accordance with the Adler formulation of Eq. (21), we can identify the corresponding Lorentz structures and group the results as

$$\begin{aligned} A^{\alpha\mu,3}_{(c)} + A^{\alpha\mu,3}_{(e)} + A^{\alpha\mu,3}_{(g)} + A^{\alpha\mu,3}_{(i)} &= \sqrt{\frac{2}{3}}\Big[g_3(q^2)\left(g^{\alpha\mu}\gamma\cdot q - q^\alpha\gamma^\mu\right) + g_4(q^2)\left(q\cdot p'g^{\alpha\mu} - q^\alpha p'^\mu\right)\\ &\quad + g_5(q^2)g^{\alpha\mu} + g_6(q^2)q^\alpha q^\mu\Big]. \quad (31)\end{aligned}$$

It is interesting to note that these loop results depend only on known masses and couplings: m_π, M_N, M_Δ, f_π, g_A, h_A, and H_A. Here, we adopt the following values: $m_\pi = 0.139\,\mathrm{GeV}$, $M_N = 0.939\,\mathrm{GeV}$, $M_\Delta = 1.232\,\mathrm{GeV}$, $f_\pi = 0.0924\,\mathrm{GeV}$, $g_A = 1.267$, $h_A = 2.85$, and $H_A = (9/5)g_A$. The value of H_A is obtained from large N_c relations and its uncertainty is discussed below. In other words, the q^2 dependence of the loop functions are

genuine predictions of the present work, in contrast with the $\delta^{(2)}$ and $\delta^{(3)}$ tree level diagrams, which contain basically unknown low energy constants: d_1, d_2, d_3, d_4, f_1, f_2, f_3, f_4, f_5, f_6, and f_7. Some of these LEC, (d_3, d_4, f_5, f_7), also appear in pion-nucleon scattering and could, in principle, be extracted from there [44].

Apart from diagrams (a), (c), (e), (g), and (i), the external axial source can also couple to a pion and interact through it with the system. These are the so-called pion pole terms (diagrams (b), (d), (f), (h), and (j)) and are calculated below.

The Lagrangian responsible for the coupling of the external axial source with the pion at second order is

$$\mathcal{L}^{(2)} = -f_\pi \partial_\mu \pi^a a^{a,\mu}. \tag{32}$$

With this and the low-energy counter terms given above, we can easily write down the pion-pole contributions:

$$A^{\alpha\mu,3}_{\rm pion-pole} = \sqrt{\frac{2}{3}}\frac{q^\alpha q^\mu}{q^2-m_\pi^2}\left[\frac{h_A}{2} + d_3\gamma\cdot q + \frac{d_4}{M_\Delta}p'\cdot q - f_2 q^2 - \frac{f_5}{M_\Delta}p'\cdot q\gamma\cdot q \right.$$
$$\left. -\frac{f_7}{M_\Delta^2}(p'\cdot q)^2 - (g_5 + g_6 q^2)\right] \tag{33}$$

with g_5 and g_6 the loop functions calculated above.

IV. RESULTS AND DISCUSSIONS

In this section, we present our results for the form factors in terms of the LEC and the loop functions g_3, g_4, g_5, and g_6 (Table I). It should be mentioned that the Partially Conserved Vector Current (PCAC) relation

$$C_5^A + \frac{C_6^A}{M_N^2}q^2|_{m_\pi\to 0} = 0 \tag{34}$$

holds up to every order in our χPT study, which can be easily checked from Table I.

As mentioned above, the one-loop results are free of unknown couplings, but the LEC are basically not known. Since these LEC always appear in particular combinations, we can introduce $\tilde{d}_1 = d_1 - (f_4+f_6)\Delta$, $\tilde{d}_2 = d_2 - f_3\Delta$, and $\tilde{d}_3 = d_3 + d_4 - (f_5+f_7)\Delta$ and treat them as free parameters. Therefore, effectively, we have five unknown constants: $\tilde{d}_1$, $\tilde{d}_2$, $\tilde{d}_3$, f_1, and f_2.

From Table I, we can conclude that

TABLE I: The axial transition form factors in relativistic baryon chiral perturbation theory; d_1, d_2, d_3, d_4 are order 2 LEC (in units of GeV^{-1}) while f_1, f_2, f_3, f_4, f_5, f_6, f_7 are order 3 LEC (in units of GeV^{-2}); $g_3(q^2)$, $g_4(q^2)$, $g_5(q^2)$, and $g_6(q^2)$ are the one-loop contributions as defined by Eq. (31).

FF	$\delta^{(1)}$	$\delta^{(2)}$	$\delta^{(3)}$
$-\sqrt{\frac{3}{2}}\frac{C_3^A(q^2)}{M_N}$	0	$-d_2$	$f_3\Delta + g_3(q^2)$
$-\sqrt{\frac{3}{2}}\frac{C_4^A(q^2)}{M_N^2}$	0	$-d_1/M_\Delta$	$(f_4+f_6)\Delta/M_\Delta + g_4(q^2)$
$-\sqrt{\frac{3}{2}}C_5^A(q^2)$	$-\frac{h_A}{2}$	$-(d_3+d_4)\Delta$	$(f_5+f_7)\Delta^2 + (f_1+f_2)q^2 + g_5(q^2)$
$-\sqrt{\frac{3}{2}}\frac{C_6^A(q^2)}{M_N^2}$	$\frac{h_A/2}{q^2-m_\pi^2}$	$\frac{(d_3+d_4)\Delta}{q^2-m_\pi^2}$	$-f_1 + g_6(q^2) + \frac{-(f_5+f_7)\Delta^2 - f_2 q^2 - (g_5(q^2)+g_6(q^2)q^2)}{q^2-m_\pi^2}$

(a) At order $\delta^{(1)}$, $C_3^A = 0$, $C_4^A = 0$, and $C_5^A = \sqrt{\frac{2}{3}}\frac{h_A}{2} \approx 1.16$ with $h_A = 2.85$ from Ref. [46], which is determined from the Δ-resonance width, $\Gamma_\Delta = 0.115\,\mathrm{GeV}$. Furthermore, C_6^A is related to C_5^A through the pion-pole mechanism, i.e.,

$$C_6^A = C_5^A \frac{M_N^2}{m_\pi^2 - q^2}. \tag{35}$$

(b) At order $\delta^{(2)}$, C_3^A, C_4^A, and C_5^A receive a finite constant contribution. The above relation, Eq. (35), between C_5^A and C_6^A still holds.

(c) At order $\delta^{(3)}$, the LEC give constant contributions to all form factors, and q^2 dependent contributions to C_5^A and C_6^A. The one-loop diagrams start at this order.

Before presenting the loop results we specify our regularization procedure due to the complications with the power counting mentioned in Section II.A. The loops are regularized in the $\overline{MS}$ scheme, subtracting in addition the real part of the contribution to the form factors at q^2=0. Since there is no counter terms linear in q^2 at $\delta^{(2)}$, this procedure guarantees to recover the power counting in all form factors.

We show in Fig. 2 the one-loop contributions to the form factors C_3^A, C_4^A, C_5^A, and C_6^A (except the pion-pole diagrams which only contribute to C_6^A). One can see that only diagrams c, d (N-N) and g, h (Δ-N) from Fig. 1 contribute to the imaginary part of the form

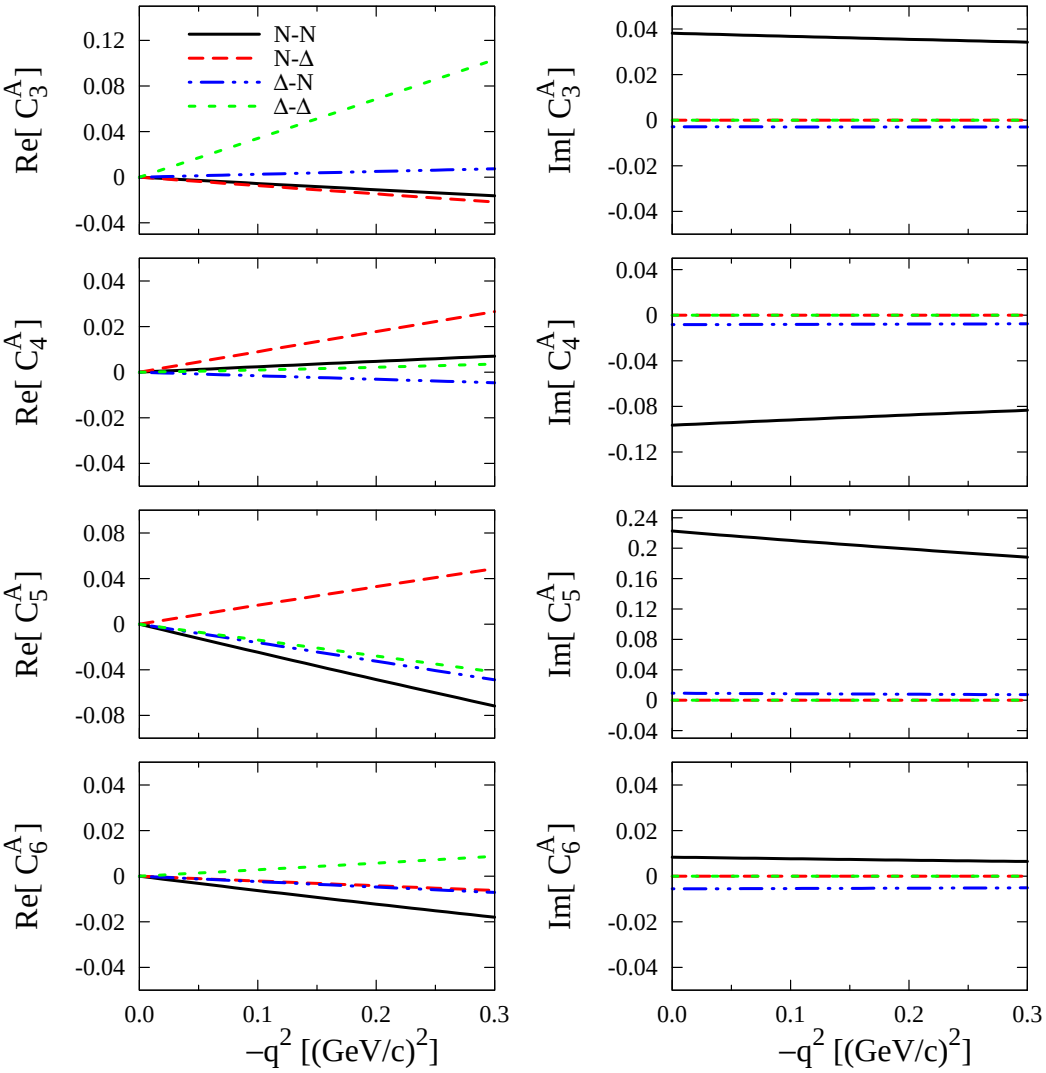

FIG. 2: (Color online) One-loop contributions to the form factors C_3^A, C_4^A, C_5^A, and C_6^A. The pion-pole diagrams, which only contribute to C_6^A, have not been included. The N-N, N-Δ, Δ-N, Δ-Δ labels denote the contributions of diagrams with nucleon-nucleon, nucleon-Delta, Delta-nucleon, Delta-Delta internal lines.

factors, with N-N being dominant. One also finds that C_4^A and C_6^A receive relatively small corrections from the one-loop calculation, whereas C_3^A gets a relatively large one coming from the Δ-Δ diagrams (diagrams i, j). This seemingly large q^2 dependence, however, suffers from the uncertainty related to the $\pi\Delta\Delta$ coupling H_A because the Δ-Δ loop contribution is proportional to H_A^2.

In Fig. 3, the loop contributions from all diagrams to each form factor are added. Clearly,

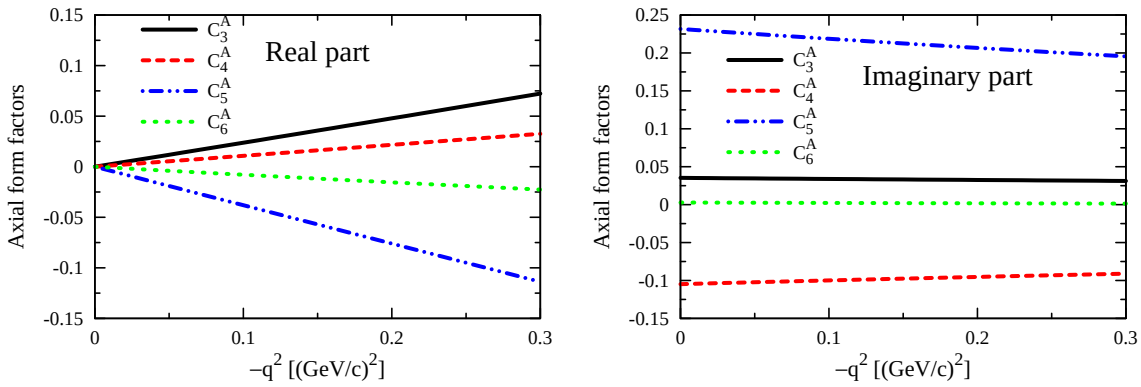

FIG. 3: (Color online) One-loop contributions to the form factors C_3^A, C_4^A, C_5^A, and C_6^A. The pion-pole diagrams, which only contribute to C_6^A, have not been included

one can see that C_5^A has the largest imaginary part; C_4^A the second; next is the C_3^A, and C_6^A receives the smallest contribution.

Without the one-loop contributions, C_6^A can be easily separated into a non-pole part and a pion-pole part, i.e.,

$$C_6^A = -\tilde{g}_{\pi N\Delta} M_N^2 \sqrt{\frac{2}{3}} \left[\frac{1}{q^2 - m_\pi^2} + \frac{1}{6} r_A^2 \right] \tag{36}$$

with

$$\tilde{g}_{\pi N\Delta} = \frac{h_A}{2} + \tilde{d}_3 \Delta - f_2 m_\pi^2, \tag{37}$$

$$r_A^2 = -\frac{6}{\tilde{g}_{\pi N\Delta}} (f_1 + f_2) \approx 6 \frac{d}{dq^2} \log(C_5^A)|_{q^2=0}. \tag{38}$$

This is equivalent to the HBχPT result of Ref. [42]

$$r_A^2 = -\frac{6}{\Lambda_x^2} \frac{1}{g_{\pi N\Delta}} \left[\frac{\tilde{b_3} + \tilde{b_8}}{2} \frac{\Lambda_x}{M_N} + c_2 \right], \tag{39}$$

with the correspondence $\tilde{g}_{\pi N\Delta} = g_{\pi N\Delta}$ and $(f_1 + f_2) = \frac{1}{\Lambda_x^2} \left[\frac{\tilde{b_3} + \tilde{b_8}}{2} \frac{\Lambda_x}{M_N} + c_2 \right]$.

V. COMPARISON WITH OTHER APPROACHES

A. Phenomenological fits

Bubble chamber neutrino data have been used to extract information about the axial $N \to \Delta$ form factors [4, 9, 52, 53]. However, there are some important limitations. First, the cross section is basically dominated by the C_5^A form factor and shows very little sensitivity to

$C^A_{3,4,6}$. Second, the statistics is quite low and, furthermore, the two available data sets from BNL [9] and ANL [7] are clearly different. Finally, it is difficult to disentangle the Δ from other background pion production processes [3, 4]. Therefore, all these works make some additional assumptions. A set of them often found in the literature[6] is: C^A_3=0, $C^A_4 = -\frac{1}{4}C^A_5$, and C^A_6 is related to C^A_5 through Eq. (35). In this way only C^A_5 is fitted to the experiment. As an example, we can take Kitagaki et al. [9] where it has the following functional form:

$$C^A_5(q^2) = C^A_5(0)\left[1 - \frac{a_5 q^2}{b_5 - q^2}\right]\left(1 - \frac{q^2}{M_A^2}\right)^{-2} \tag{40}$$

with $C^A_5(0) = 1.2$, $a_5 = -1.21$, $b_5 = 2$ GeV^2, and M_A is fitted to data yielding $M_A = 1.28^{+0.08}_{-0.10}$ GeV. We will refer to this set of form factors as Kitagaki-Adler (KA) form factors.

As we have shown above, there are 5 independent parameters in the δ expansion scheme up to chiral order 3: $\tilde{d}_1$, $\tilde{d}_2$, $\tilde{d}_3$, f_1 and f_2. We fix them in such a way that the real part of our form factors reproduces many of the features of the KA ones. To obtain $C^A_3 = 0$, we set $\tilde{d}_2 = 0$; therefore its contribution comes only from loop calculations which are of chiral order 3. Strictly speaking , Eq. (35) is not fulfilled at order $\delta^{(3)}$ but, if one neglects the small loop contributions, it can be satisfied by taking $f_1 = 0$. Correspondingly, the relation $C^A_4(0) = -\frac{1}{4}C^A_5(0)$ fixes $\tilde{d}_1$; $C^A_5(0) = 1.2$ fixes $\tilde{d}_3$. The only LEC left, f_2, is then fixed to reproduce $\frac{\partial C^A_5}{\partial q^2}$ at $q^2 = 0$.

The results obtained this way are shown in Fig. 4, with the following parameter values $\tilde{d}_1 = -0.514$ GeV^{-1}, $\tilde{d}_2 = 0$, $\tilde{d}_3 = 0.153$ GeV^{-1}, $f_1 = 0$, and $f_2 = -2.184$ GeV^{-2}. One can clearly see that the calculated C^A_5 and C^A_6 are in good agreement with the KA form factors. On the other hand, the q^2 dependence of C^A_4 is much weaker that the one assumed in KA, $C^A_4 = -\frac{C^A_5}{4}$, and we cannot accommodate their results at order $\delta^{(3)}$. For C^A_3, the q^2 dependence is also very weak (compared to C^A_5). In Fig. 4, the dark shadowed area indicates a modification of M_A within its uncertainties as given in Ref. [9]. As we mentioned above, the C^A_3 dependence on q^2 is rather sensitive to the coupling constant H_A. This can be easily seen from the light shadowed area in the upper-left panel of Fig. 4, which covers the region of $g_A \leq H_A \leq (9/5)g_A$. The form factors, $C^A_{4,5,6}$, on the other hand, are less sensitive to the value of H_A.

[6] This choice originates from the analysis of Refs. [1, 54] of Adler's results obtained using dispersion relations [55].

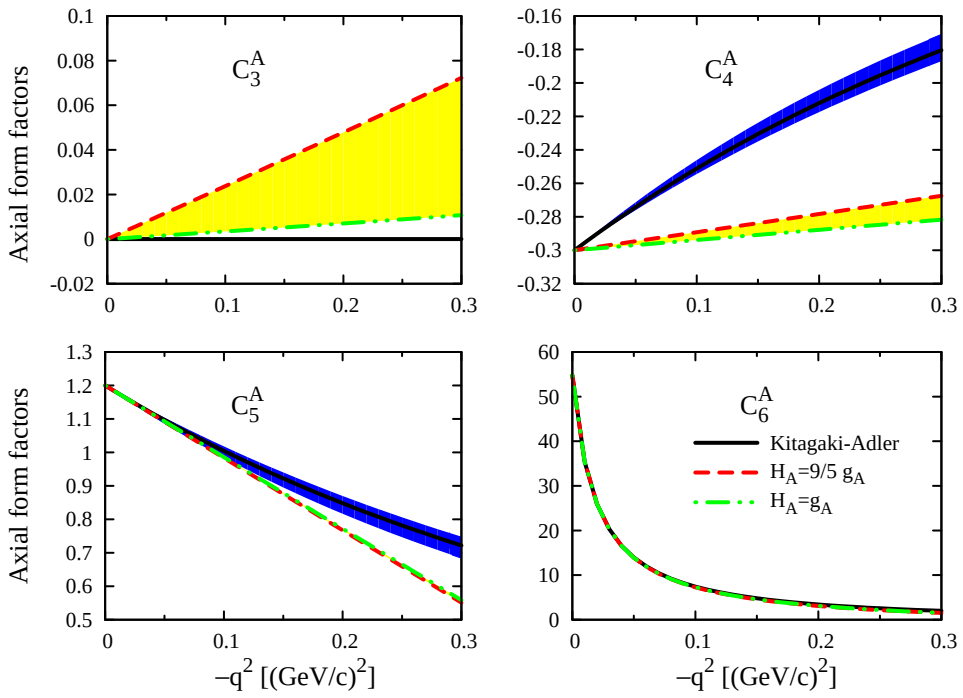

FIG. 4: (Color online) Comparison with the Kitagaki-Adler form factors. The dark shadowed area indicates the uncertainty of $M_A = 1.28^{+0.08}_{-0.10}\,\mathrm{GeV}$ as determined in Ref. [9]. The light shadowed area indicates the sensitivity of the results to the $\pi\Delta\Delta$ coupling H_A, which covers $H_A = (9/5)g_A$ to $H_A = g_A$.

A word of caution is in place about the comparison of C_3^A and C_4^A with the KA form factors. In χPT, the leading order counter terms linear in q^2 contributing to C_3^A and C_4^A appear at chiral order 4. A fair comparison with the phenomenological fits (particularly the q^2 dependence) should, in principle, be done at order 4. However, the $\delta^{(3)}$ χPT results might give us a clue on the magnitude of the q^2 dependence of C_3^A and C_4^A. Furthermore, if we believe in the phenomenological assumption, or the results of other approaches, the difference between the third order χPT results and the results of other approaches might help us estimate the value of the corresponding fourth order LEC. Indeed, the upper panels of Fig. 4 indicate that small $\delta^{(4)}$ corrections $h_i q^2$ with *natural* values for the LEC h_i can reproduce the slope assumed for C_3^A and C_4^A by the KA ansatz.

We also notice that a recent analysis [4] obtained a smaller value for $C_5^A(0)$ by including non Δ contributions and fitting to the low invariant mass ANL data. In the present χPT study, we do have the higher-order contributions, $\tilde{d}_3$, which could alter $C_5^A(0)$ within such

a range; however, the same LEC appear in pion-nucleon scattering processes. A combined analysis is mandatory to determine whether one can accommodate the small $C_5^A(0)$ obtained in, for instance, Ref. [4]. This is left for future studies.

B. Quark models

There have been many studies of the $N \to \Delta$ axial transition form factors in various quark models, both relativistic and non-relativistic. For a brief review of quark model studies, we refer the readers to Refs. [10, 11]. Compared to dynamical model studies, a feature of most quark model calculations is that the obtained form factors are real due to time-reversal symmetry, while in dynamical models, like our χPT study, these form factors are in general complex due to the opening of the pion-nucleon channel.

Quark model results are in fact quite scattered. Taking, for instance, the models discussed in Ref. [11], we observed that the prediction of $C_5^A(0)$ runs from 0.81 to 1.53, $C_4^A(0)$ runs from -0.66 to 0.14 and $C_3^A(0)$ runs from 0 to 0.05. These models also obtain the non-pole part of C_6^A whose value at $q^2 = 0$ ranges from -0.72 to 1.13. We could use these results to extract our constants although the large differences between them do not allow to reach solid conclusions about their values. From $C_5^A(0)$ one gets $\tilde{d}_3$, and from its slope $\partial C_5^A/\partial q^2$ at $q^2 = 0$, $(f_1 + f_2)$. This fixes the non-pole part of $C_6^A(0)$ (neglecting the one-loop corrections) since

$$C_6^{A(\mathrm{non-pole})}(0) \approx \sqrt{\frac{2}{3}} M_N^2 (f_1 + f_2)\,, \tag{41}$$

which is nothing but a direct consequence of PCAC. Using the quark model calculation of Ref. [11] for C_5^A we obtain $C_6^{A(\mathrm{non-pole})}(0) \approx -2$. This value is almost a factor three larger in magnitude than the one obtained directly from that model in spite of the fact that it implements PCAC at the quark level by introducing one- and two-body axial exchange currents.

Analogously, we can use quark model results for C_3^A and C_4^A at $q^2 = 0$ to obtain $\tilde{d}_1$ and $\tilde{d}_2$. The smallness of $C_3^A(0)$ predicted by all calculations points towards a $\tilde{d}_2$ close to zero, in agreement with the phenomenological assumption. The situation is much more uncertain with $\tilde{d}_1$, both in sign and magnitude. In Fig. 5, the q^2 dependence of the real parts of C_3^A and C_4^A in our calculation, which at order $\delta^{(3)}$ is dictated by the loops, is compared to several quark models. As in the case of the KA form factors discussed above, we can expect from

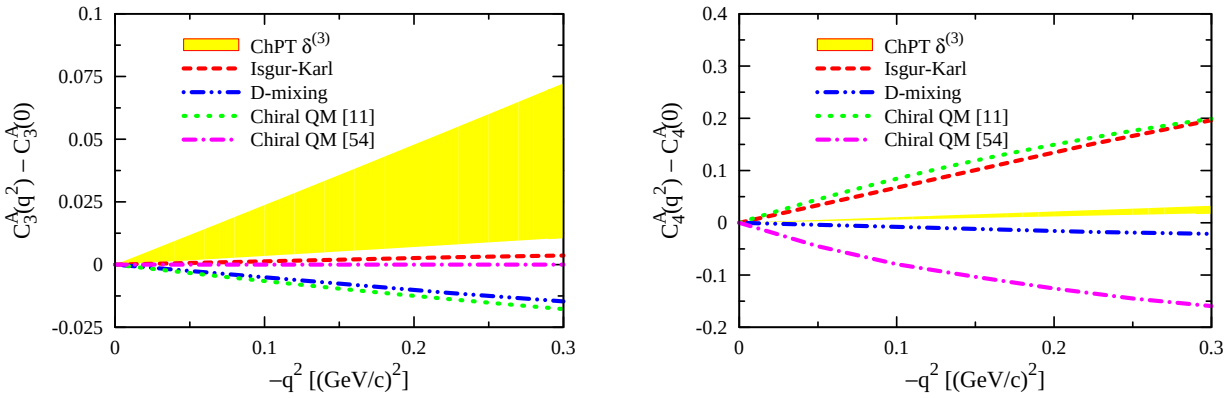

FIG. 5: (Color online) Comparison with the non relativistic Isgur-Karl and D-mixing quark model results of Ref. [10], and those of the chiral quark models of Refs. [11] and [56].

this comparison that next order terms linear in q^2 with small (*natural*) values of the LEC are sufficient to eliminate the discrepancies in the low q^2 behavior with any of these quark models.

C. Lattice QCD results

Recently, the $N \to \Delta$ axial transition form factors have been studied in lattice QCD [13, 14]. Some major conclusions are (i) C_3^A and C_4^A are suppressed compared to C_5^A and C_6^A, and (ii) C_5^A can be described by a dipole ansatz $C_5^A(0)/(1+Q^2/M_A^2)^2$ but with a smaller $C_5^A(0)$ and a larger M_A ($\gtrsim 1.5$ GeV), compared to the Kitagaki-Adler form factors. These results should be taken with caution because of the still relatively large pion mass (≥ 350 MeV) used in the study.

In principle, χPT is the perfect tool to extrapolate the lattice QCD results to the physical region. Meanwhile, one can also fix the unknown couplings to the lattice QCD results. Due to the regularization method we used and the fact that the lattice data points are still scarce, we will leave this subject to the future.

VI. SUMMARY AND CONCLUSIONS

We have studied the axial $N \to \Delta$ transition form factors up to one-loop order in relativistic baryon chiral perturbation theory with the δ expansion scheme. The adopted Lagrangians

including the $\Delta(1232)$ are *consistent*, i.e., spin-3/2 gauge symmetric, which automatically decouples unphysical spin-1/2 fields. Consequently, our results do not depend on the specific value of the gauge-fixing parameter that is present in the most general spin-3/2 propagator, and avoid various problems related to inconsistent couplings.

The form factor C_5^A exhibits the richest structure in our study. It receives contributions starting at chiral order 1, at which we find that $C_5^A(0) = \sqrt{\frac{2}{3}}\frac{h_A}{2} \approx 1.16$ for $h_A = 2.85$. At higher orders, this value is modified by low energy constants that are unknown but which also appear in pion-nucleon scattering. At chiral order 3, this form factor gets q^2 dependent contributions, some of them complex. Actually, we find that C_5^A has the largest imaginary part among the four form factors. We also obtain that, up to chiral order 2, $C_6^A = C_5^A \frac{M_N^2}{m_\pi^2 - q^2}$. At order 3, C_6^A has a non-pole contribution whose value at $q^2 = 0$ is related to the slope of C_5^A at $q^2 = 0$. Assuming natural values for the LEC, this non-pole part is small compared to the dominant pion-pole mechanism.

Both C_3^A and C_4^A start at chiral order 2 and get their q^2 dependence at order 3 from the loops. For C_3^A, we find a small q^2 dependence, which is quite sensitive to the $\pi\Delta\Delta$ coupling constant, H_A. On the other hand, its imaginary part, coming mainly from the N-N internal diagram, is finite (~ 0.03 at $q^2 = 0$) and has a mild q^2 dependence. This suggests that C_3^A is small (compared to $C_{4,5,6}^A$) but not necessarily zero. The C_4^A dependence on q^2 is also found to be rather mild at order $\delta^{(3)}$.

We have compared our results with a phenomenological set of form factors used in the analysis of neutrino-induced pion production data and also with different quark model calculations. They could be used to extract the low energy constants but the scarcity of data and the large differences between quark model results make it difficult to come to solid conclusions. In the case of C_3^A and specially C_4^A, the comparison should, in principle, be done at order 4 where corresponding leading order counter terms linear in q^2 appear. Nevertheless we can say that reasonable agreement with all these approaches can be obtained with natural values of the LEC.

Future experiments with electron and neutrino beams, combined with the analysis of pion-nucleon scattering data, can shed more light on these form factors. The extrapolation of lattice QCD results to the physical region should also be pursued.

VII. ACKNOWLEDGMENTS

We thank Mauro Napsuciale, Stefan Scherer, Wolfram Weise, and in particular Massimiliano Procura and Vladimir Pascalutsa for useful discussions. We are also grateful to Eliecer Hernandez for providing us with the results of several quark model calculations. L. S. Geng acknowledges financial support from the Ministerio de Educacion y Ciencia in the Program "Estancias de doctores y tecnologos extranjeros". J. Martin Camalich acknowledges the same institution for a FPU fellowship. This work was partially supported by the MEC contract FIS2006-03438, the Generalitat Valenciana ACOMP07/302, and the EU Integrated Infrastructure Initiative Hadron Physics Project contract RII3-CT-2004-506078.

Note added in proof: After submitting this paper, a new preprint [57] appeared that studies the $N \to \Delta$ axial form factors up to one-loop order in HBChPT using the small scale expansion scheme. Within this framework, there is no q^2 dependence coming from the loop-functions. This supports the smooth q^2 dependences found in the present work. Namely, the q^2 dependence of the loops in our relativistic framework is counted as of higher-order in HBChPT.

---

[1] C. H. Llewellyn Smith, Phys. Rept. **3**, 261 (1972).

[2] G. L. Fogli and G. Nardulli, Nucl. Phys. **B160**, 116 (1979).

[3] T. Sato, D. Uno, and T. S. H. Lee, Phys. Rev. **C67**, 065201 (2003).

[4] E. Hernandez, J. Nieves, and M. Valverde, Phys. Rev. **D76**, 033005 (2007).

[5] L. Alvarez-Ruso, L. S. Geng, and M. J. Vicente Vacas, Phys. Rev. **C76**, 068501 (2007).

[6] S. J. Barish et al., Phys. Rev. **D19**, 2521 (1979).

[7] G. M. Radecky et al., Phys. Rev. **D25**, 1161 (1982).

[8] T. Kitagaki et al., Phys. Rev. **D34**, 2554 (1986).

[9] T. Kitagaki et al., Phys. Rev. **D42**, 1331 (1990).

[10] J. Liu, N. C. Mukhopadhyay, and L.-s. Zhang, Phys. Rev. **C52**, 1630 (1995).

[11] D. Barquilla-Cano, A. J. Buchmann, and E. Hernandez, Phys. Rev. **C75**, 065203 (2007).

[12] T. M. Aliev, K. Azizi, and A. Ozpineci, Nucl. Phys. **A799**, 105 (2008).

[13] C. Alexandrou, T. Leontiou, J. W. Negele, and A. Tsapalis, Phys. Rev. Lett. **98**, 052003

(2007).

[14] C. Alexandrou, G. Koutsou, T. Leontiou, J. W. Negele, and A. Tsapalis, Phys. Rev. **D76**, 094511 (2007).

[15] S. P. Wells et al. (G0 Collaboration), JLAB experiment No. E97-104 (1997).

[16] N. C. Mukhopadhyay, M. J. Ramsey-Musolf, S. J. Pollock, J. Liu, and H. W. Hammer, Nucl. Phys. **A633**, 481 (1998).

[17] S.-L. Zhu, C. M. Maekawa, B. R. Holstein, and M. J. Ramsey-Musolf, Phys. Rev. Lett. **87**, 201802 (2001).

[18] M. Hasegawa et al. (K2K), Phys. Rev. Lett. **95**, 252301 (2005).

[19] J. L. Raaf (BooNE), Nucl. Phys. Proc. Suppl. **139**, 47 (2005).

[20] M. O. Wascko (MiniBooNE), Nucl. Phys. Proc. Suppl. **159**, 79 (2006).

[21] K. B. M. Mahn, Nucl. Phys. Proc. Suppl. **159**, 237 (2006).

[22] D. Drakoulakos et al. (Minerva) (2004), hep-ex/0405002.

[23] D. S. Ayres et al. (NOvA) (2004), hep-ex/0503053.

[24] S. Weinberg, Physica **A96**, 327 (1979).

[25] J. Gasser and H. Leutwyler, Nucl. Phys. **B250**, 465 (1985).

[26] G. Ecker, Prog. Part. Nucl. Phys. **35**, 1 (1995).

[27] S. Scherer, Adv. Nucl. Phys. **27**, 277 (2003).

[28] J. Gasser, M. E. Sainio, and A. Svarc, Nucl. Phys. **B307**, 779 (1988).

[29] E. E. Jenkins and A. V. Manohar, Phys. Lett. **B255**, 558 (1991).

[30] V. Bernard, N. Kaiser, and U.-G. Meissner, Int. J. Mod. Phys. **E4**, 193 (1995).

[31] T. Becher and H. Leutwyler, Eur. Phys. J. **C9**, 643 (1999).

[32] J. Gegelia, G. Japaridze, and X. Q. Wang, J. Phys. **G29**, 2303 (2003).

[33] T. Fuchs, J. Gegelia, G. Japaridze, and S. Scherer, Phys. Rev. **D68**, 056005 (2003).

[34] T. R. Hemmert, B. R. Holstein, and J. Kambor, J. Phys. **G24**, 1831 (1998).

[35] V. Pascalutsa and D. R. Phillips, Phys. Rev. **C68**, 055205 (2003).

[36] V. Bernard, T. R. Hemmert, and U.-G. Meissner, Phys. Lett. **B565**, 137 (2003).

[37] C. Hacker, N. Wies, J. Gegelia, and S. Scherer, Phys. Rev. **C72**, 055203 (2005).

[38] G. C. Gellas, T. R. Hemmert, C. N. Ktorides, and G. I. Poulis, Phys. Rev. **D60**, 054022 (1999).

[39] T. A. Gail and T. R. Hemmert, Eur. Phys. J. **A28**, 91 (2006).

[40] V. Pascalutsa and M. Vanderhaeghen, Phys. Rev. Lett. **95**, 232001 (2005).

[41] V. Pascalutsa and M. Vanderhaeghen, Phys. Rev. **D73**, 034003 (2006).

[42] S.-L. Zhu and M. J. Ramsey-Musolf, Phys. Rev. **D66**, 076008 (2002).

[43] V. Pascalutsa, M. Vanderhaeghen, and S. N. Yang, Phys. Rept. **437**, 125 (2007).

[44] N. Fettes and U. G. Meissner, Nucl. Phys. **A679**, 629 (2001).

[45] V. Pascalutsa, Phys. Lett. **B503**, 85 (2001).

[46] V. Pascalutsa and M. Vanderhaeghen, Phys. Lett. **B636**, 31 (2006).

[47] P. A. Schreiner and F. Von Hippel, Nucl. Phys. **B58**, 333 (1973).

[48] J. A. M. Vermaseren (2000), math-ph/0010025.

[49] R. Mertig, M. Bohm, and A. Denner, Comput. Phys. Commun. **64**, 345 (1991).

[50] G. J. van Oldenborgh and J. A. M. Vermaseren, Z. Phys. **C46**, 425 (1990).

[51] T. Hahn and M. Perez-Victoria, Comput. Phys. Commun. **118**, 153 (1999).

[52] L. Alvarez-Ruso, S. K. Singh, and M. J. Vicente Vacas, Phys. Rev. **C59**, 3386 (1999).

[53] O. Lalakulich and E. A. Paschos, Phys. Rev. **D71**, 074003 (2005).

[54] J. Bijtebier, Nucl. Phys. **B21**, 158 (1970).

[55] S. L. Adler, Ann. Phys. **50**, 189 (1968).

[56] B. Golli, S. Sirca, L. Amoreira, and M. Fiolhais, Phys. Lett. **B553**, 51 (2003).

[57] M. Procura (2008), arXiv: 0803.4291 [hep-ph].

[58] V. A. Smirnov (2006), *Feynman Integral Calculus*, Berlin, Germany: Springer.

VIII. APPENDIX

A. Isospin transition matrices and antisymmetric Gamma matrix products

The isospin 1/2 to 3/2 and 3/2 to 3/2 transition matrices T^a and $\mathcal{T}^a$ appearing in the $N\Delta$ and $\Delta\Delta$ Lagrangians are given by:

$$T^1 = \frac{1}{\sqrt{6}} \begin{pmatrix} -\sqrt{3} & 0 & 1 & 0 \\ 0 & -1 & 0 & \sqrt{3} \end{pmatrix}, \tag{42}$$

$$T^2 = \frac{-i}{\sqrt{6}} \begin{pmatrix} \sqrt{3} & 0 & 1 & 0 \\ 0 & 1 & 0 & \sqrt{3} \end{pmatrix}, \tag{43}$$

$$T^3 = \sqrt{\frac{2}{3}} \begin{pmatrix} 0 & 1 & 0 & 0 \\ 0 & 0 & 1 & 0 \end{pmatrix}. \tag{44}$$

$$\mathcal{T}^1 = \frac{2}{3} \begin{pmatrix} 0 & \sqrt{3}/2 & 0 & 0 \\ \sqrt{3}/2 & 0 & 1 & 0 \\ 0 & 1 & 0 & \sqrt{3}/2 \\ 0 & 0 & \sqrt{3}/2 & 0 \end{pmatrix}, \tag{45}$$

$$\mathcal{T}^2 = \frac{2i}{3} \begin{pmatrix} 0 & -\sqrt{3}/2 & 0 & 0 \\ \sqrt{3}/2 & 0 & -1 & 0 \\ 0 & 1 & 0 & -\sqrt{3}/2 \\ 0 & 0 & \sqrt{3}/2 & 0 \end{pmatrix}, \tag{46}$$

$$\mathcal{T}^3 = \begin{pmatrix} 1 & 0 & 0 & 0 \\ 0 & 1/3 & 0 & 0 \\ 0 & 0 & -1/3 & 0 \\ 0 & 0 & 0 & -1 \end{pmatrix}. \tag{47}$$

The totally antisymmetric Gamma matrix products appearing in the *consistent* $N\Delta$ and $\Delta\Delta$ Lagrangians are defined as:

$$\gamma^{\mu\nu} = \frac{1}{2}[\gamma^\mu, \gamma^\nu], \tag{48}$$

$$\gamma^{\mu\nu\rho} = \frac{1}{2}\{\gamma^{\mu\nu}, \gamma^\rho\} = -i\varepsilon^{\mu\nu\rho\sigma}\gamma_\sigma\gamma_5, \tag{49}$$

$$\gamma^{\mu\nu\rho\sigma} = \frac{1}{2}[\gamma^{\mu\nu\rho}, \gamma^\sigma] = i\varepsilon^{\mu\nu\rho\sigma}\gamma_5 \tag{50}$$

with the following conventions: $g^{\mu\nu} = \mathrm{diag}(1, -1, -1, -1)$, $\varepsilon_{0,1,2,3} = -\varepsilon^{0,1,2,3} = 1$, $\gamma_5 = i\gamma_0\gamma_1\gamma_2\gamma_3$.

B. Loop functions

In the calculation of the loop diagrams, we have used the following d-dimensional integrals in Minkowski space:

$$\int d^dk \frac{k^{\alpha_1}\ldots k^{\alpha_{2n}}}{(\mathcal{M}^2 - k^2)^\lambda} = i\pi^{d/2}\frac{\Gamma(\lambda - n + \epsilon - 2)}{2^n\Gamma(\lambda)}\frac{(-1)^n g_s^{\alpha_1\ldots\alpha_{2n}}}{(\mathcal{M}^2)^{\lambda-n+\epsilon-2}} \tag{51}$$

with $g_s^{\alpha_1\ldots\alpha_{2n}} = g^{\alpha_1\alpha_2}\ldots g^{\alpha_{2n-1}\alpha_{2n}} + \ldots$ a combination symmetrical with respect to the permutation of any pair of indices (with $(2n-1)!!$ terms in the sum) [58].

The $\mathcal{M}^2$ that appear in the calculation of the N-N, N-Δ, Δ-N, and Δ-Δ internal diagrams are, respectively,

$$\mathcal{M}^2_{NN} = x\, m_\pi^2 - x(1-x-y)M_\Delta^2 + (1-x-xy)M_N^2 - y(1-x-y)q^2 - i\epsilon, \tag{52}$$

$$\mathcal{M}^2_{N\Delta} = x\, m_\pi^2 + (1-x)(1-x-y)M_\Delta^2 + y(1-x)M_N^2 - y(1-x-y)q^2 - i\epsilon, \tag{53}$$

$$\mathcal{M}^2_{\Delta N} = x\, m_\pi^2 + (x^2+xy-x+y)M_\Delta^2 + (1-x-y-xy)M_N^2 - y(1-x-y)q^2 - i\epsilon, \tag{54}$$

$$\mathcal{M}^2_{\Delta\Delta} = x\, m_\pi^2 + (1-2x+x^2+xy)M_\Delta^2 - xyM_N^2 - y(1-x-y)q^2 - i\epsilon, \tag{55}$$

where x and y are Feynman parameters.

C. Feynman parameterization integrals

We present below the loop integrals, diagrams (c), (e), (g) and (i) of Fig. 1, cast in the Feynman parameterization. We use the following notation: $\widetilde{C}_i^{(XY)}$ is the $\overline{MS}$-regularized contribution of the loop to C_i^A with X and Y being the baryons in the internal line (in this order), $\bar{\mathcal{M}}^2_{XY}$=$\mathcal{M}^2_{XY}/M_\Delta^2$, $r = M_N/M_\Delta$, $\mu_\pi = m_\pi/M_\Delta$, and $\bar{Q}^{2n} = Q^{2n}/M_\Delta^{2n}$ (with $Q^2 = -q^2$).

The couplings are contained in the constants $\mathcal{C}_{XY}$:

$$\mathcal{C}_{NN} = 2\sqrt{\frac{2}{3}}\,\frac{g_A^2 h_A M_\Delta^2}{128 f_\pi^2 \pi^2} \;\; ; \;\; \mathcal{C}_{N\Delta} = \frac{5}{3}\sqrt{\frac{2}{3}}\,\frac{g_A h_A H_A M_\Delta^2}{192 f_\pi^2 \pi^2} \;\; ;$$
$$\mathcal{C}_{\Delta N} = \frac{1}{3}\sqrt{\frac{2}{3}}\,\frac{h_A^3 M_\Delta^2}{192 f_\pi^2 \pi^2} \;\; ; \;\; \mathcal{C}_{\Delta\Delta} = \frac{10}{9}\sqrt{\frac{2}{3}}\,\frac{h_A H_A^2 M_\Delta^2}{576 f_\pi^2 \pi^2}\,.$$

Then, the expressions of the loop functions are:

$$
\begin{aligned}
\widetilde{C}_3^{(NN)} &= -\frac{\mathcal{C}_{NN}}{24} r(14r+3) + r\,\mathcal{C}_{NN} \int_0^1 dx \int_0^{1-x} dy \Big\{ \Big[y\left(\left(-3y + x\left(y^2+2y-1\right)+1\right) r^3 \right. \\
&+ \left((y-1)x^2 + \left(y^2-y-1\right)x - 3y + 2\right) r^2 - x(y+3)(x+y-1)r + x\left(-x^2 - 2yx \right. \\
&+ \left. x - y^2 + y\right) + \bar{Q}^2 (x+y-1)\left((y-1)(x+y) + r\left(y^2+2y-1\right)\right)\Big) \Big] \frac{1}{\bar{\mathcal{M}}_{NN}^2} \\
&- \left[2y(2y-1) + x(4y-1) + r\left(4y^2+5y-1\right) \right] \log\left(\bar{\mathcal{M}}_{NN}^2\right) \Big\}, \\
\widetilde{C}_4^{(NN)} &= \frac{r^2\,\mathcal{C}_{NN}}{6} - 2\,r^2\,\mathcal{C}_{NN} \int_0^1 dx \int_0^{1-x} dy\, y \Big\{ \Big[\left(-3y + x\left(y^2+y-2\right)+2\right) r^2 - 2x(x \\
&+ y-1)r - y(x+y-1)\left((1-y)\bar{Q}^2 + x\right) \Big] \frac{1}{\bar{\mathcal{M}}_{NN}^2} - 2(2y-1)\log\left(\bar{\mathcal{M}}_{NN}^2\right) \Big\}, \\
\widetilde{C}_5^{(NN)} &= -\frac{1-r}{r}\widetilde{C}_3^{(NN)} - \frac{1-r^2-\bar{Q}^2}{2\,r^2}\widetilde{C}_4^{(NN)} - 2\,r\,\mathcal{C}_{NN} \int_0^1 dx \int_0^{1-x} dy\, ((1-r)y + r + x) \times \\
&\times \log\left(\bar{\mathcal{M}}_{NN}^2\right), \\
\widetilde{C}_6^{(NN)} &= \frac{r^2\,\mathcal{C}_{NN}}{6} - 2\,r^2\,\mathcal{C}_{NN} \int_0^1 dx \int_0^{1-x} dy\, y \Big\{ \Big[y((x(y-1) - 2y + 1)r^2 + 2(x+y-1)r \\
&- x(x+y-1) + \bar{Q}^2(y-1)(x+y-1)) \Big] \frac{1}{\bar{\mathcal{M}}_{NN}^2} - 2(2y-1)\log\left(\bar{\mathcal{M}}_{NN}^2\right) \Big\}. \\
\widetilde{C}_3^{(N\Delta)} &= \frac{\mathcal{C}_{N\Delta}}{288} r\left(-39{\mu_\pi}^2 + 155r^2 + 27\bar{Q}^2 + 96r - 69\right) - r\,\mathcal{C}_{N\Delta} \int_0^1 dx \int_0^{1-x} dy\ \times \\
&\times \Big\{ y \Big[x(x(y-1) - 2y + 1)yr^4 + y\left(-2x^2 - 3yx + x + 1\right) r^3 + \left((1-2y)x^3 + (3-2y)yx^2 \right. \\
&+ \left. \left(y^2-1\right)x + y\right) r^2 + x\left(2x^2 + 5yx + 3y^2 - y - 2\right) r + x(x+1)\left(x^2 + (2y-1)x \right. \\
&+ \left. (y-1)y\right) + \bar{Q}^4(y-1)y\left(x^2 + (2y-1)x + (y-1)y\right) + \bar{Q}^2\left((1-2y)x^3 + \left(2(y-1)r^2 \right.\right. \\
&- \left. 2r - 4y + 3\right) yx^2 + \left(2\left(r^2-1\right)y^3 + \left(-5r^2 - 5r + 1\right)y^2 + \left(2r^2 + r + 2\right)y - 1\right)x \\
&+ \left. y\left(\left(y - 2y^2\right)r^2 + \left(-3y^2 + 2y + 1\right)r - (y-1)^2\right)\right) \Big] \frac{1}{\bar{\mathcal{M}}_{N\Delta}^2} - \Big[(4 - 33y)x^2 + \left(33\left(r^2 \right.\right. \\
&+ \left. \left. \bar{Q}^2 - 1\right)y^2 - \left(21r^2 + 32r + 21\bar{Q}^2 - 5\right)y + 4\right)x + y\left((13 - 32y)r^2 + (8 - 48y)r - 16y \right. \\
&+ \left. \bar{Q}^2\left(33y^2 - 38y + 13\right) + 8\right) \Big] \frac{\log\left(\bar{\mathcal{M}}_{N\Delta}^2\right)}{4} + 13(4y-1)\frac{\bar{\mathcal{M}}_{N\Delta}^2 \log\left(\bar{\mathcal{M}}_{N\Delta}^2\right)}{4} \Big\},
\end{aligned}
$$

$$
\begin{aligned}
\widetilde{C}_4^{(N\Delta)} &= -\frac{r^2\,\mathcal{C}_{N\Delta}}{240}\left(-45{\mu_\pi}^2+27r^2+33\bar{Q}^2-152r-55\right)+r^2\,\mathcal{C}_{N\Delta}\int_0^1 dx\int_0^{1-x} dy\;\times\\
&\times\;\Big\{y\Big[(3x(x(y-1)-2y+1)yr^4-y\left((y+3)x^2+5yx-3\right)r^3+\left((2-5y)x^3+(9-5y)yx^2\right.\\
&+\;\left.\left(5y^2-y-2\right)x+y\right)r^2+x\left((y+4)x^2+y(y+8)x+5y^2-y-4\right)r+3\bar{Q}^4(y\\
&-\;1)y\left(x^2+(2y-1)x+(y-1)y\right)+x\left(2x^3+4yx^2+\left(2y^2+y-2\right)x+(y-1)y\right)\\
&-\;\bar{Q}^2\left((5y-2)x^3+y\left(-6(y-1)r^2+(y+3)r+10y-7\right)x^2+\left(\left(-6r^2+r+5\right)y^3\right.\right.\\
&+\;\left.\left.\left(15r^2+7r-4\right)y^2-3\left(2r^2+1\right)y+2\right)x+y\left(3y(2y-1)r^2+\left(5y^2-2y-3\right)r\right.\right.\\
&+\;\left.\left.(y-1)^2\right)\right)\Big]\frac{1}{2\bar{\mathcal{M}}_{N\Delta}^2}+\Big[(19y-2)x^2+\left(\left(-24r^2+5r-24\bar{Q}^2+19\right)y^2+\left(15r^2+14r\right.\right.\\
&+\;\left.\left.15\bar{Q}^2-5\right)y-2\right)x+y\left(3(8y-3)r^2+4(5y+1)r+4y-3\bar{Q}^2\left(8y^2-9y+3\right)-2\right)\Big]\times\\
&\times\;\frac{\log\left(\bar{\mathcal{M}}_{N\Delta}^2\right)}{2}+(4y-1)\frac{9\bar{\mathcal{M}}_{N\Delta}^2\,\log\left(\bar{\mathcal{M}}_{N\Delta}^2\right)}{2}\Big\}\,,\\
\widetilde{C}_5^{(N\Delta)} &= -\frac{1-r}{r}\,\widetilde{C}_3^{(N\Delta)}-\frac{1-r^2-\bar{Q}^2}{2\,r^2}\,\widetilde{C}_4^{(N\Delta)}+\frac{\mathcal{C}_{N\Delta}}{1440}\left(5\left(-27\bar{Q}^2+9(43-3r)r+158\right){\mu_\pi}^2\right.\\
&+\;\left.99\bar{Q}^4+5\bar{Q}^2(r(36r-191)-57)+r(r(r(81r+385)+135)+5175)+290\right)\\
&-\;\mathcal{C}_{N\Delta}\int_0^1 dx\int_0^{1-x} dy\,\Big\{\Big[\left((r-1)^2+\bar{Q}^2\right)y\left((y-1)y(x+y-1)(x+y)\bar{Q}^4\left((1\right.\right.\\
&-\;\left.\left.2y)x^3+(2r(r(y-1)-1)-4y+3)yx^2+\left(y\left((y(2y-5)+2)r^2-5yr+r-2y^2+y\right.\right.\right.\right.\\
&+\;\left.\left.\left.\left.2)-1\right)x+y\left(-(r+1)(2r+1)y^2+(r(r+2)+2)y+r-1\right)\right)\bar{Q}^2+(r-1)(r+1)^2\times\right.\\
&\times\;\left.(r(x-2)-x-1)xy^2+x(r(r+2)+x)\left(x^2-1\right)-(r+1)\left(-xr^3-r^2+2(r-1)x^3\right.\right.\\
&+\;\left.\left.\left(r\left(r^2+r-4\right)-1\right)x^2+x\right)y\right)\Big]\frac{3}{4\bar{\mathcal{M}}_{N\Delta}^2}-\Big[x^3+4r^2x^2+2rx^2+6x^2+6r^2x-2rx-x\\
&-\;4r^2+(r-1)^2(r+1)(24r(x-1)-23x-12)y^2+8r-(r-1)\left(-9r^3+4r^2+2r\right.\\
&+\;\left.(25r-22)x^2+3(r(r(5r+6)-5)+2)x+6\right)y+3\bar{Q}^4y(y(8y-9)+x(8y-5)+3)\\
&-\;\bar{Q}^2\left((25y-4)x^2+(y(2y+r(6r(5-8y)+47y+3)+13)-6)x+y\left(-3(y(8y-17)\right.\right.\\
&+\;\left.\left.6)r^2+(y(47y-8)+13)r+(41-23y)y-22\right)+4\right)\Big]\frac{\log\left(\bar{\mathcal{M}}_{N\Delta}^2\right)}{4}-\Big[4(x-8y+5)\\
&+\;9\bar{Q}^2(1-4y)+r(9r(1-4y)+68y+7)\Big]\frac{\bar{\mathcal{M}}_{N\Delta}^2\,\log\left(\bar{\mathcal{M}}_{N\Delta}^2\right)}{4}\Big\}\,,\\
\widetilde{C}_6^{(N\Delta)} &= -\frac{r^2\,\mathcal{C}_{N\Delta}}{360}(199r+3)+r^2\,\mathcal{C}_{N\Delta}\int_0^1 dx\int_0^{1-x} y\,dy\,\Big\{y\Big[((r-2)r+x)(x-1)^2+\left(r^2+r\right.\\
&-\;\left.2\right)(r-x)y(x-1)+(r-1)^2(r+1)xy^2-\bar{Q}^2(x+y-1)(x(y-1)-y(r+(r-1)y\right.\\
&+\;\left.2)+1)\Big]\frac{1}{2\bar{\mathcal{M}}_{N\Delta}^2}+\Big[(x+y-1)(5y-2)-5ry(y+1)\Big]\frac{\log\left(\bar{\mathcal{M}}_{N\Delta}^2\right)}{2}\Big\}\,.
\end{aligned}
$$

$$
\begin{aligned}
\widetilde{C}_3^{(\Delta N)} &= \frac{r\,\mathcal{C}_{\Delta N}}{1440}\left(5(73r+95){\mu_\pi}^2+2\bar{Q}^2(11r+54)+r(r(345r+467)+175)+359\right)\\
&+ r\,\mathcal{C}_{\Delta N}\int_0^1 dx\int_0^{1-x} dy\left\{\Big[\left((r+1)^2+\bar{Q}^2\right)y(x+y-1)\left(x(y-1)^2r^3-\left(y+x\left(y^2\right.\right.\right.\right.\\
&+ \left.\left.\left.\left.x(y-1)\right)-1\right)r^2+\left(\bar{Q}^2(x+y-1)(y-1)^2+y+x(-yx+x-(y-2)y+1)\right.\right.\right.\\
&- \left.\left.\left.1\right)r+(x+y-1)\left(x^2+\left(-y\bar{Q}^2+\bar{Q}^2+y+1\right)x-\bar{Q}^2y^2\right)\right)\Big]\frac{1}{4\bar{\mathcal{M}}_{\Delta N}^2}-\Big[\left(2x\left(4y^2\right.\right.\right.\\
&- \left.\left.\left.6y+1\right)+(y-1)(y(5y-4)+1)\right)r^3+\left(5y^3-(x+17)y^2+(9-2x(3x+5))y\right.\\
&+ \left.2x^2+x-1\right)r^2+\left((3-13y)x^2+2(2-9y)yx+y(12-y(5y+7))\right)r+(x-5y\\
&+ 1)(x+y)^2-2(r+x-2y)+2\bar{Q}^2(x+y-1)\left((4r-3)y^2-(6r+3x+2)y+r+x\right)\Big]\times\\
&\times \frac{\log\left(\bar{\mathcal{M}}_{\Delta N}^2\right)}{4}-(x+r(2-3y)+y+1)\bar{\mathcal{M}}_{\Delta N}^2\log\left(\bar{\mathcal{M}}_{\Delta N}^2\right)\Big\},\\
\widetilde{C}_4^{(\Delta N)} &= -\frac{r^2\,\mathcal{C}_{\Delta N}}{720}\left(120{\mu_\pi}^2+8\bar{Q}^2+r(175r+107)+190\right)+r^2\,\mathcal{C}_{\Delta N}\int_0^1 dx\int_0^{1-x} dy\,\times\\
&\times \left\{\Big[y(x+y-1)\left(-xy(x+y-1)r^4+(y+x(x+(x+2)y-1)-1)r^3+\left(x\left(2y^2+4xy\right.\right.\right.\right.\\
&+ \left.\left.\left.\left.(x-2)x-2\right)+\bar{Q}^2\left(y\left(-y^2-4xy+y-2(x-2)x+1\right)-1\right)\right)r^2+\left(-y+\bar{Q}^2\left((x\right.\right.\right.\right.\\
&+ \left.\left.\left.\left.2)y^2+x(x+4)y-3y+(x-4)x+1\right)-x(2y+x(x+y+3))+1\right)r+x-\bar{Q}^4y(x\right.\\
&+ \left.y-1)(x+2y-2)-x(y+(x+y)(2x+y))+\bar{Q}^2\left(x^3+(5y-3)x^2+(y(5y-4)\right.\right.\\
&+ \left.\left.1)x+y\left(y^2+y-2\right)\right)\Big]\frac{1}{2\bar{\mathcal{M}}_{\Delta N}^2}-\Big[x^3+\left(\left(17-6\bar{Q}^2\right)y-3\right)x^2+\left(y\left(2\bar{Q}^2(9-11y)\right.\right.\\
&+ \left.\left.21y-8)+1\right)x+r\left((5x+8)y^2+x(5x+14)y-7y+(x-4)x+1\right)+r^2\left(y\left(-6x^2\right.\right.\right.\\
&+ \left.\left.\left.4(3-4y)x+(3-5y)y+3)-1\right)+y\left(5y(y+1)-4\bar{Q}^2(y(4y-7)+3)-6\right)\Big]\frac{\log\left(\bar{\mathcal{M}}_{\Delta N}^2\right)}{2}\right.\\
&- \left.2(x+6y-2)\bar{\mathcal{M}}_{\Delta N}^2\log\left(\bar{\mathcal{M}}_{\Delta N}^2\right)\right\},\\
\widetilde{C}_5^{(\Delta N)} &= -\frac{1-r}{r}\,\widetilde{C}_3^{(\Delta N)}-\frac{1-r^2-\bar{Q}^2}{2\,r^2}\,\widetilde{C}_4^{(\Delta N)}-\frac{\mathcal{C}_{\Delta N}}{1440}\left(5\left(5\bar{Q}^2+r(26r+63)+5\right){\mu_\pi}^2+8\bar{Q}^4\right.\\
&+ \left.\bar{Q}^2\left(42r^2+52r+15\right)+r(r(r(193r+289)+114)+223)+7\right)-\mathcal{C}_{\Delta N}\int_0^1 dx\int_0^{1-x} dy\,\times\\
&\times \left\{\Big[\left(y^2-\left(x^2+2\right)y+1\right)r^4+\left(y+x\left(y^2+(x-2)y+x+2\right)-1\right)r^3+\left(x^3-2\bar{Q}^2(x\right.\right.\\
&- \left.\left.1)yx-\left(2\bar{Q}^2x+x+2\right)y^2+2y\right)r^2-(x+y-1)\left(x^2-\left(\bar{Q}^2+\left(\bar{Q}^2-1\right)y+1\right)x\right.\right.\\
&- \left.\left.\bar{Q}^2y^2\right)r+\left(\bar{Q}^2+1\right)(x+y-1)\left(\left(\bar{Q}^2+1\right)y+(x+y)\left(x-\bar{Q}^2y\right)\right)\Big]\frac{\log\left(\bar{\mathcal{M}}_{\Delta N}^2\right)}{4}\right.\\
&+ \left.\left(x+r((r-1)x-y)+y+\bar{Q}^2(x+y-1)-1\right)\bar{\mathcal{M}}_{\Delta N}^2\log\left(\bar{\mathcal{M}}_{\Delta N}^2\right)\right\},
\end{aligned}
$$

$$
\begin{aligned}
\widetilde{C}_6^{(\Delta N)} &= -\frac{r^2\,\mathcal{C}_{\Delta N}}{720}\left(95{\mu_\pi}^2+16\bar{Q}^2+r(121r+91)+199\right)-r^2\,\mathcal{C}_{\Delta N}\int_0^1 dx\int_0^{1-x} dy\,\times\\
&\times\ \Big\{\Big[y(x+y-1)\left((y-1)(xy+y-1)r^4+x((y-4)y+3)r^3+\left(2\left(x^2+x+y\right)\right.\right.\\
&-\ \left.y\left(4x^2+3yx+2y\right)+\bar{Q}^2(y-1)\left(y^2+2xy-1\right)\right)r^2+\left(\bar{Q}^2\left((y-1)^2+x(y-3)\right)(y\right.\\
&-\ \left.1)+y-x(x(y-5)+(y-4)y+1)-1\right)r+3x^3+x^2\left(\bar{Q}^2(2-4y)+5y-1\right)\\
&+\ (y-1)y\left((y-1)\bar{Q}^4-2y\bar{Q}^2+1\right)+x\left(\left(\left(\bar{Q}^2-6\right)\bar{Q}^2+2\right)y^2-\left(\bar{Q}^2-6\right)\bar{Q}^2y+y\right.\\
&-\ \left.\bar{Q}^{\,2}-1\right)\Big)\Big]\frac{1}{2\bar{\mathcal{M}}_{\Delta N}^2}+\Big[\left(y\left((2x(3-5y)+y(3-5y)+3)r^2+(x(18-5y)+(13-5y)y\right.\right.\\
&-\ \left.7)r+10(x+y)(2x+y)-6(3x+y)-2\bar{Q}^2(x+y-1)(5y-3)\right)-(r+x)(r+2x\\
&-\ \left.1))\Big]\frac{\log\left(\bar{\mathcal{M}}_{\Delta N}^2\right)}{2}+2(5y-1)\bar{\mathcal{M}}_{\Delta N}^2\log\left(\bar{\mathcal{M}}_{\Delta N}^2\right)\Big\}.\\
\widetilde{C}_3^{(\Delta\Delta)} &= \frac{r\,\mathcal{C}_{\Delta\Delta}}{1440}\left(6620{\mu_\pi}^4+\left(368\bar{Q}^2+7(483-320r)r+22011\right){\mu_\pi}^2+182\bar{Q}^4+\bar{Q}^2(2520\right.\\
&-\ \left.r(274r+3))+r(r(r(648r-625)-7941)+3789)+32345)+r\,\mathcal{C}_{\Delta\Delta}\int_0^1 dx\int_0^{1-x} dy\,\times\\
&\times\ \Big\{\Big[\left((r+1)^2+\bar{Q}^2\right)y(x+y-1)\left(x^4+2\left(\bar{Q}^2+(r-1)r-\left(r^2+\bar{Q}^2\right)y+y+1\right)x^3\right.\\
&+\ \Big(\left.(y-2)y\bar{Q}^4+\left(2(y-2)yr^2+(2y-1)r-4y^2+2y-1\right)\bar{Q}^2-(r-2)r^2+\left(r^2-1\right)^2y^2\right.\\
&-\ \left.2r\left((r-1)r^2+2\right)y+2(r+2y-1)\right)x^2+\left(2\bar{Q}^4y(y-1)^2+(r-1)\left((2(y-1)y-1)r^2\right.\right.\\
&-\ \left.(y+1)r-2y^2+y+3\right)+\bar{Q}^2\left(2r^2y(y-1)^2+r(4(y-1)y-1)+y(3-2y(y+1))\right.\\
&-\ \left.3))\,x+\bar{Q}^2(y-1)y\left(\left(\bar{Q}^2(y-1)-2\right)y+r(2y-1)\right)\right)\Big]\frac{1}{4\bar{\mathcal{M}}_{\Delta\Delta}^2}-\Big[(xy(x(18y-19)\\
&+\ 4(y(3y-7)+3))r^4+\left(10(2x+1)y^3+(x(20x-19)-12)y^2+2(1-6x)xy-6y\right.\\
&-\ \left.2x(x+2)+4\right)r^3+\left(2(5-14y)x^3+(4(5-8y)y+6)x^2+(y((7-4y)y+19)-20)x\right.\\
&-\ \left.11y+5y^2(2y-3)+8\right)r^2-\left(10(2x+1)y^3+\left(40x^2+x-4\right)y^2+x(4x+1)(5x-4)y\right.\\
&-\ \left.18y-2x((x-1)x+6)+8\right)r+10x^4+(7-10y)y^2+23y+x^3(12y+7)-2x^2(3(y\\
&-\ 3)y+19)+\bar{Q}^4y(x+y-1)(3y(6y-5)+x(18y-19)+5)+x\left(y\left(-8y^2+y-27\right)\right.\\
&+\ \left.31)+\bar{Q}^2\left(2(5-14y)x^3+(8(1-6y)y+2)x^2+y(77-6y(2y+7))x-26x-39y\right.\right.\\
&+\ \left.y^2(8(y-5)y+67)+r^2y\left((36y-38)x^2+4(4y(3y-5)+9)x+(y-1)^2(12y-5)\right)\right.\\
&+\ \left.r\left(2(2y(5y-3)-1)x^2+(5y-2)(y(8y-5)+2)x+(y-1)y(y(20y-9)+11)+4\right)\right.\\
&+\ \left.12)-12)\Big]\frac{\log\left(\bar{\mathcal{M}}_{\Delta\Delta}^2\right)}{4}-\Big[\left(28x+66y+\bar{Q}^2\left(-88y^2+76y+x(38-88y)-28\right)\right.\right.\\
&-\ \left.2\left((5y(3y-5)+x(44y-19)+7)r^2+(4x(5y-1)+2y(10y-9)+7)r-(39x-5y)\right.\right.\times\\
&\times\ \left.(x+y))-67)\Big]\frac{\bar{\mathcal{M}}_{\Delta\Delta}^2\log\left(\bar{\mathcal{M}}_{\Delta\Delta}^2\right)}{4}-14\,\bar{\mathcal{M}}_{\Delta\Delta}^4\log\left(\bar{\mathcal{M}}_{\Delta\Delta}^2\right)\Big\},
\end{aligned}
$$

$$
\begin{aligned}
\widetilde{C}_4^{(\Delta\Delta)} &= -\frac{r^2\,\mathcal{C}_{\Delta\Delta}}{720}\left(2340{\mu_\pi}^4+3\left(72\bar{Q}^2+(269-130r)r+2261\right){\mu_\pi}^2+60\bar{Q}^4+\bar{Q}^2(788-r(42r\right.\\
&+ 23))+r(r(r(90r+43)-1288)+1289)+8988)-r^2\,\mathcal{C}_{\Delta\Delta}\int_0^1 dx\int_0^{1-x} dy\,\times\\
&\times\left\{\left[y(x+y-1)\left(\left(5\bar{Q}^2+r(5r-2)-1\right)x^4+\left((4-8y)\bar{Q}^4+(14y+2r(r(4-8y)+y)\right.\right.\right.\\
&+ 1)\bar{Q}^2-(r+1)(2y+r(2r(-5y+r(4y-2)+2)-5)+3)\Big)x^3+\left(3(y-1)yr^6-yr^5\right.\\
&+ \left(-7y^2+y+3\right)r^4+(3-6y)r^3+(y(5y+9)-4)r^2+7yr+r+\bar{Q}^4(r(9r(y-1)-1)\\
&- 19y+11)y+3\bar{Q}^6(y-1)y-y(y+7)+\bar{Q}^2\left(9(y-1)yr^4-2yr^3+(2(6-13y)y+3)r^2\right.\\
&- 6yr+r+y(13y+7)-7)-1)x^2+\left(3y(y(2y-3)+1)\bar{Q}^6+\left(y\left(6(y(2y-3)+1)r^2\right.\right.\right.\\
&+ \left.\left.\left.2\left(y^2+y-2\right)r+(5-14y)y+7\right)-4\right)\bar{Q}^4+\left(2(r+1)^2(r(3r-5)+2)y^3+(10\right.\\
&- r(r(r(9r-8)+3)+10))y^2+(r-1)\left(3r^3-7r^2+r+8\right)y-5r^2+r-3\Big)\bar{Q}^2+\left(r^2\right.\\
&- \left.\left.1\right)\left(6(y-1)yr^3+\left(-4y^2+y-1\right)r^2+3\left(-2y^2+y+1\right)r+4y^2-1\right)\right)x+\bar{Q}^2(y-1)\times\\
&\times\left.y\left(3(y-1)y\bar{Q}^4+\left(3(y-1)yr^2+(2y(y+2)-3)r-y(3y+5)+1\right)\bar{Q}^2+4y+r(-6y\right.\right.\\
&+ \left.\left.r(-4y+r(6y-3)-1)+1)+1)\right)\right]\frac{1}{2\bar{\mathcal{M}}_{\Delta\Delta}^2}-\Big[\left(3xy\left(10y^2+14xy-16y-9x+6\right)r^4\right.\\
&+ y\left(6(x+5)y^2+(33-4x)xy-42y-4x(x+7)+12\right)r^3+\left(-2(23x+10)y^3-6\left(19x^2\right.\right.\\
&+ \left.\left.x-3\right)y^2+x\left(-68x^2+46x+31\right)y-12y+2x(x(7x+5)-9)+4\right)r^2+\left(-6(x+5)y^3\right.\\
&+ (x-1)(10x-33)y^2+(x(x(16x-29)+28)-1)y+4x^2+6x-4\Big)r+4(4x+5)y^3\\
&+ \left(46x^2+44x-17\right)y^2+2(x-1)x(x(7x+9)-9)+x(4x(11x+7)-49)y+13y\\
&+ 3\bar{Q}^4y(x+y-1)(y(14y-13)+x(14y-9)+3)+\bar{Q}^2\left(2(7-34y)x^3+2\left(y\left(3(14y-9)r^2\right.\right.\right.\\
&- \left.\left.\left.2(y+1)r-82y+35)+2\right)x^2+\left(y\left(6(y(19y-26)+9)r^2+(y(14y+23)-20)r+4(11\right.\right.\right.\\
&- \left.\left.\left.31y)y+53)-26\right)x+y\left(3(y-1)(2y-1)(5y-3)r^2+(y(y(18y+11)-40)+17)r\right.\right.\\
&+ \left.\left.y(57-4y(7y+3))-29)+8)-4\right)\right]\frac{\log\left(\bar{\mathcal{M}}_{\Delta\Delta}^2\right)}{2}+\Big[\left(-16x-62y+12\bar{Q}^2(y(13y-12)\right.\\
&+ x(13y-4)+3)+2\left(3(2y(5y-6)+x(26y-8)+3)r^2-(10yx+x-(3y+5)(5y-2))r\right.\\
&- \left.\left.(x+y)(53x+25y))+39\right)\Big]\frac{\bar{\mathcal{M}}_{\Delta\Delta}^2\log\left(\bar{\mathcal{M}}_{\Delta\Delta}^2\right)}{2}-36\bar{\mathcal{M}}_{\Delta\Delta}^4\log\left(\bar{\mathcal{M}}_{\Delta\Delta}^2\right)\Big\}\,,\\
\widetilde{C}_5^{(\Delta\Delta)} &= -\frac{1-r}{r}\,\widetilde{C}_3^{(\Delta\Delta)}-\frac{1-r^2-\bar{Q}^2}{2\,r^2}\,\widetilde{C}_4^{(\Delta\Delta)}+\frac{\mathcal{C}_{\Delta\Delta}}{1440}\left(20\left(117\bar{Q}^2+r(117r-272)+117\right){\mu_\pi}^4\right.\\
&+ \left(216\bar{Q}^4+(2(370-87r)r+7263)\bar{Q}^2+r\left(r\left(-390r^2+2012r+3773\right)-15462\right)\right.\\
&+ \left.7047\right){\mu_\pi}^2+60\bar{Q}^6+\bar{Q}^4(r(18r-109)+930)+\bar{Q}^2\left(r\left(48r^3-717r+37\right)+11013\right)\\
&+ r(r(r(r(r(90r-347)-803)+5067)+3238)-21462)+10143)+\mathcal{C}_{\Delta\Delta}\int_0^1 dx\int_0^{1-x} dy\,\times
\end{aligned}
$$

$$
\begin{aligned}
&\times \left\{ \left[\left(r^4 + 2\left(\bar{Q}^2 - 1\right) r^2 + \left(\bar{Q}^2 + 1\right)^2 \right) y(x + y - 1) \left(x^4 + \left(r^2 + \bar{Q}^2 - 2\left(r^2 + \bar{Q}^2 - 1 \right) y + 1 \right) x^3 \right.\right. \\
&+ \left((y-1) y r^4 + \left(-2y^2 + 2\bar{Q}^2 (y-1) y + 1 \right) r^2 - 2yr + r + y \left(\bar{Q}^2 \left(\bar{Q}^2 (y-1) - 4y + 2 \right) + y + 3 \right) \right. \\
&- \left.\left. 1 \right) x^2 + \left(y(y(2y-3)+1)\bar{Q}^4 + \left(y \left((y(2y-3)+1) r^2 + 2(y-1) r - y(2y+1) + 2 \right) - 1 \right) \bar{Q}^2 \right. \\
&+ \left. (r-1)((r+1)(2r(y-1) - 2y + 1) y + 1)) x + \bar{Q}^2 (y-1) y \left(\left(\bar{Q}^2 (y-1) - 2 \right) y + r(2y \right. \right. \\
&- \left.\left. 1))) \right] \frac{3}{4 \bar{\mathcal{M}}_{\Delta\Delta}^2} - \left[\left(11x^3 r^4 + 8x^2 r^4 - 9x r^4 - 6x^3 r^3 + 20x r^3 - 4r^3 + 10x^4 r^2 + 9x^3 r^2 - 12x^2 r^2 \right.\right. \\
&- \left. x r^2 + 4r^2 - 10x^4 r - 4x^3 r + 32x^2 r - 12xr + 4r + 10x^4 + 10x^3 + 2(r-1)^3 (r+1)^2 ((15r \right. \\
&+ \left. 16)x + 15) y^3 - 18x^2 + (r-1)^2 (r+1) \left(6x(7x-8) r^3 + \left(30x^2 + x - 42 \right) r^2 + 3\left(-20x^2 + x \right.\right.\right. \\
&- \left.\left.\left. 4 \right) r - 54x^2 + 4x + 31 \right) y^2 + 2x - (r-1) \left(9x(3x-2) r^5 + 2(x(10x+9) - 6) r^4 + (x(x(52x \right. \\
&- \left. 31) + 7) - 6) r^3 + \left(x \left(30x^2 - 9x - 8 \right) + 9 \right) r^2 + \left(x \left(-30x^2 + 9x + 20 \right) + 6 \right) r + 4(11 - 3x) x^2 \right. \\
&+ \left. x + 3 \right) y + 3\bar{Q}^6 y(x + y - 1)(y(14y - 13) + x(14y - 9) + 3) + \bar{Q}^4 \left((11 - 52y) x^3 + (y(-30y \right. \\
&+ \left. r(-12y + 9r(14y - 9) + 7) - 7) + 2) x^2 + \left(y \left(6(11y(3y-4) + 15) r^2 + ((71 - 24y) y - 38) r \right. \right. \right. \\
&+ \left.\left.\left. (y-1)(96y - 113)) - 17 \right) x + y \left(18(y-1)(r - 2ry)^2 + y(y(74y - 191) + 147) + 2r(11 \right. \right. \\
&- \left.\left. 2y(y(3y - 16) + 17)) - 34) + 4) + \bar{Q}^2 \left(3y \left(3(14y - 9) x^2 + 4(y(12y - 17) + 6) x + (y-1)(2y \right. \right. \right. \\
&- \left.\left.\left. 1)(5y - 3)) r^4 + 2y \left((7 - 12y) x^2 + ((60 - 11y) y - 37) x + y(y(y + 39) - 54) + 17 \right) r^3 + (2(11 \right. \right. \\
&- \left.\left. 52y) x^3 + 2((22 - 81y) y + 5) x^2 - (y(y(120y + 23) - 76) + 26) x + y(y((33 - 62y) y + 21) \right. \right. \\
&- \left.\left. 14) + 4) r^2 + \left((22y - 6) x^3 + \left(42y^2 - 34y + 2 \right) x^2 + (y(2y(9y + 32) - 79) + 26) x - (y-1) \times \right. \right. \\
&\times \left.\left. (y(2(y - 45) y + 51) - 12)) r + (x + y - 1) \left(32y^3 - 4(13x + 27) y^2 - x(74x + 41) y + 22y \right. \right. \\
&+ \left.\left. x(2x + 5)(5x + 3))) - 4) \right] \frac{\log\left(\bar{\mathcal{M}}_{\Delta\Delta}^2 \right)}{4} - \left[\left(48x r^4 - 18r^4 - 26x r^3 + 38r^3 + 86x^2 r^2 + 36x r^2 \right.\right. \\
&- \left. 21r^2 - 82x^2 r - 16xr + 65r + 86x^2 - 10(r-1)^2 (r+1)(6r+7) y^2 + 38x - 2(r-1)(8x \right. \\
&+ \left. r(-28x + r(32x + 6r(13x - 6) + 3) + 6) + 67) y - 12\bar{Q}^4 (y(13y - 12) + x(13y - 4) + 3) \right. \\
&+ \left. \bar{Q}^2 \left(-6\left(9(1 - 2y)^2 + 4x(13y - 4) \right) r^2 + 2\left(46y^2 - 66y + x(46y - 13) + 22 \right) r - 226y^2 \right. \right. \\
&+ \left.\left. 86x(x + 1) - 140xy + 278y - 75) - 39) \right] \frac{\bar{\mathcal{M}}_{\Delta\Delta}^2 \log\left(\bar{\mathcal{M}}_{\Delta\Delta}^2 \right)}{4} - 2\left(9\bar{Q}^2 + r(9r - 8) + 9 \right) \times \right. \\
&\times \left. \bar{\mathcal{M}}_{\Delta\Delta}^4 \log\left(\bar{\mathcal{M}}_{\Delta\Delta}^2 \right) \right\},
\end{aligned}
$$

$$
\begin{aligned}
\widetilde{C}_6^{(\Delta\Delta)} &= -\frac{r^2\,\mathcal{C}_{\Delta\Delta}}{720}\left(5(36r+85){\mu_\pi}^2+2\left(2\bar{Q}^2(8r+23)-3r(r(34r+65)-93)-839\right)\right)\\
&+ r^2\,\mathcal{C}_{\Delta\Delta}\int_0^1 dx\int_0^{1-x} dy\left\{\left[y(1-x-y)\left(6x^4+2\left(2\left(r^2+r+\bar{Q}^2+1\right)-\left(5\bar{Q}^2+(r\right.\right.\right.\right.\\
&- 1)(5r+7)\right)y\right)x^3+\left(2\left(2\bar{Q}^4+(r(4r+3)-11)\bar{Q}^2+(r-1)^2(r+1)(2r+5)\right)y^2\\
&+ \left(-3\bar{Q}^4+(9-2r(3r+4))\bar{Q}^2-(r-1)(r+3)(r(3r+2)+4)\right)y+2\left(\bar{Q}^2(r+1)\right.\\
&+ r(r(r+2)+2)-2)\Big)x^2-\Big((r(y-1)-4y+3)y(2y-1)\bar{Q}^4+(-9y+2\,(y(y(2y-3)\\
&+ 1)r^3+y((6-5y)y-2)r^2+\left(y\left(-4y^2+2y+3\right)-1\right)r+y^2(7y+1)\right)+2\Big)\bar{Q}^2\\
&+ (r-1)\left(2\left(r^2-1\right)^2y^3-(r-1)(r+1)\left(3r^2+r+8\right)y^2+\left(r\left(r^3+10r+7\right)-6\right)y\right.\\
&- \left.2\left(r^2+r+1\right)\right)\Big)x-(y-1)y\Big(((2r(y-1)-4y+3)y-1)\bar{Q}^4+(r(y-1)-y)\,(r\\
&+ 2\left(r^2-1\right)y-9\Big)\bar{Q}^2+(r-1)^2(r+1)\Big)\Big]\frac{1}{2\bar{\mathcal{M}}_{\Delta\Delta}^2}-\Big[\left((56y-4)x^3+\left(-2\left(22\bar{Q}^2+r(22r\right.\right.\\
&+ 17)-62\right)y^2+\left(20\bar{Q}^2+4r(5r+8)-31\right)y-2(r+1)\Big)x^2+2\Big(\Big(11\bar{Q}^2(r-4)\\
&+ (r-1)(r(11r-17)-40)\Big)y^3+\left(\bar{Q}^2(47-13r)+r((30-13r)r+11)+2\right)y^2+\left(\bar{Q}^2(3r\right.\\
&- 14)+r(r(3r-10)+5)-9\Big)y-r+1\Big)x+y\left(12(r-1)^2(r+1)y^3-(r-1)(r(24r\right.\\
&+ 5)+31)y^2+r(4r(4r-3)+59)y-32y+r((3-4r)r-21)+2\bar{Q}^2(y((37-22y)y-22)\\
&+ (y-1)(y(11y-10)+2)+5)+1))\Big]\frac{\log\left(\bar{\mathcal{M}}_{\Delta\Delta}^2\right)}{2}+(7x+32y-50y(x+y)+r(y(25y\\
&- 21)+2)-4)\bar{\mathcal{M}}_{\Delta\Delta}^2\log\left(\bar{\mathcal{M}}_{\Delta\Delta}^2\right)\Big\}.
\end{aligned}
$$